Ph.D. Dissertation of Veterinary medicine

The study of neuroprotective effect of human umbilical cord blood-derived mesenchymal stem cells and herbal compound on amyotrophic lateral sclerosis

근위축성측삭경화증 동물모델에서 제대혈 유래 중간엽줄기세포와 허브 화합물의 신경보호효과에 관한 연구

August 2022

Department of Veterinary Pathobiology and preventive medicine, College of veterinary medicine, Graduate School of Seoul National University

Myung Geun Kook

The study of neuroprotective effect of human umbilical cord blood-derived mesenchymal stem cells and herbal compound on amyotrophic lateral sclerosis

By Myung Geun Kook

Submitting a Ph.D. Dissertation of Veterinary Medicine

August 2022

Graduate School of Veterinary Science
Seoul National University
Myung Geun Kook

Confirming the Ph.D. Dissertation written by
Myung Geun Kook

August 2022

Chair	박 재 학	(Seal)
Vice Chair	강 경 선	(Seal)
Examiner	윤 화 영	(Seal)
Examiner	이 승 희	(Seal)
Examiner	유 경 록	(Seal)

Abstract

The study of neuroprotective effect of human umbilical cord blood-derived mesenchymal stem cells and herbal compound on amyotrophic lateral sclerosis

Myung Geun Kook

Graduate School of Veterinary Science
Seoul National University
Myung Geun Kook

Supervisor: Kyung-Sun Kang, D.V.M., Ph.D.

Amyotrophic lateral sclerosis (ALS) is a progressive neurodegenerative disease characterized by loss of upper and lower motor neurons and degeneration of neuromuscular junctions in

skeletal muscle. Most cases of patients with ALS are sporadic ALS (sALS), while about 5−10% of patients with ALS have a family history and considered as familial ALS (fALS). The main reason of the ALS remains unknown, but several epigenetic studies have found several mutations related with the pathology of the disease. In the fALS, mutation of SOD1 which is function as free radical−scavenging enzyme Cu/Zn superoxide dismutase is wildly studied model of ALS disease. Other known genes of ALS are fused in sarcoma (FUS) gene, TAR DNA−binding protein (TARDBP), and chromosome 9 open reading frame 72 (C9orf72) (Huai & Zhang, 2019; Zou et al., 2017).

So far two drugs, Riluzole and Edaravone, have been approved by the U.S Food and Drug Administration (FDA) to cure patients with ALS. Riluzole functions as suppresser of excessive glutamate and Edaravone acts by suppressing oxidative stress. However, they provide limited improvement in survival to ALS patients (Cifra, Mazzone, & Nistri, 2013; Jaiswal, 2019; Miller, Mitchell, & Moore, 2012). Many previous studies have demonstrated several therapeutic methods that have shown positive results in ALS, including gene therapy, chemical therapy and cell therapy. In this study, the aims are to identify therapeutic efficacy of herbal compound (KCHO−1) and human umbilical cord blood−derived mesenchymal stem cells (hUCB−MSCs) for improving progression of ALS.

The KCHO-1 is a novel mixture of herbal compound that is composed of several traditional medicine and defined as complementary and alternative medicine (CAM). In this study, we identify whether oral delivery of KCHO-1 could improve disease progression and alleviate pathology in an ALS model and found that KCHO-1 effect positive on roatrod score and improve life span of SOD1 transgenic mice. Furthermore, administration of KCHO-1 inhibited reactive oxygen species (ROS) and reduced activation of gp91phox and MAP kinase activity in both microglial cells and SOD1 transgenic mice. These results demonstrate that the KCHO-1 can be a novel therapeutic option for ALS.

Among of various cell therapy, stem cell therapy is a favorable therapeutic option and has been emerged as neuroprotective in ALS disease. Furthermore, ALS is a multifactorial disease that affect various parts during disease progression (Baloh, Glass, & Svendsen, 2018; Kjaeldgaard et al., 2018). In this study, we performed administration of hUCB-MSCs in SOD1 transgenic mice repeatedly. Without route for central nervous system (CNS), we performed intramuscular infusion of hUCB-MSCs and found alleviation of pathology on the skeletal muscle of SOD1 transgenic mice. Repeat intramuscular injection of hUCB-MSCs alleviate muscle atrophy and inhibit degeneration of neuromuscular junctions through alleviation of ROS levels. Furthermore, hUCB-MSCs activate AMPK pathway in the skeletal muscle and activated AMPK induce

inhibition of the iNOS/NO signaling and upregulation of pretein synsthesis. These results demonstrate that hUCB-MSCs can improve disease progression and can be a therapeutic option and practical route for treatment of ALS.

Here we demonstrated that KCHO-1, new herbal compound, exert therapeutic effect against mutant SOD1 G93A mouse model by reducing the oxidative stress through gp91phox and MAPK pathway. Treatment of KCHO-1 also decreased activation of microglia cells depending on various concentration of KCHO-1. Furthermore, intramuscular transplantation of hUCB-MSCs significantly ameliorate muscle atrophy and denervation of ALS mouse model via activation of AMPK pathway. Consequently, we demonstrate that oral delivery of KCHO-1 and administration of hUCB-MSCs through skeletal muscle provide positive effect on ALS pathogenesis and can be promising therapeutic options for the therapy of ALS.

Keyword: Neurodegenerative disease, Amyotrophic lateral sclerosis, human umbilical cord blood derived mesenchymal stem cells, Traditional medicine, AMPK, Oxidative stress.

Student Number: 2013-21544

Published papers: Journal of veterinary science and scientific report

TABLE OF CONTENTS

ABSTRACT i

TABLE OF CONTENTS v

LIST OF ABBREVIATIONS x

LIST OF FIGURES xiii

LIST OF TABLES xvii

LITERATURE REVIEW xviii

A. Cause of ALS xviii

B. Mechanism / Pathophysiology xviii

C. Therapeutic options for ALS..... xxv

D. Therapeutics xxvii

Chapter I

A novel herbal compound, KCHO-1, reduced reactive oxygen species in the spinal cord of amyotrophic lateral sclerosis

1.1 INTRODUCTION 2
1.2 MATERIALS AND METHODS 5
1.2.1 Animals 5
1.2.2 Materials 5
1.2.3 Motor function analysis 6
1.2.4 MTT assay 6
1.2.5 Nitric oxide and ROS assay 6
1.2.6 Western blotting 7
1.2.7 Immunohistochemistry 8
1.2.8 Histology 8
1.2.9 Statistical analysis 9
1.3 RESULTS 10

1.3.1 KCHO-1 attenuated motor impairment and delayed disease onset of hSOD1^{G93A}Tg mice 10
1.3.2 KCHO-1 attenuated the death of neuronal cells in the spinal cord of hSOD1^{G93A}Tg mice 12
1.3.3 KCHO-1 attenuated the proliferation and activation of microlgial cells 15
1.3.4 KCHO-1 inhibited reactive oxigen species through gp91^{phox} and MAPK signaling 18
1.3.5 KCHO-1 inhibited reactive oxygen species in BV2 microglial cells 20
1.3.6 KCHO-1 inhibited oxidative stress in BV2 microglial cells 22
1.4 DISCUSSION 25

Chapter II

hUCB-MSCs transplanted into skeletal muscle improved motor function and survival of the SOD1 G93A mice by activating AMPK

2.1 INTRODUCTION 29
2.2 MATERIALS AND METHODS 32
2.2.1 Animals 32
2.2.2 Rotarod and disease onset 32
2.2.3 Cell culture 32
2.2.4 Immunocyto- and Immunohistochemistry 33
2.2.5 ROS assay 33
2.2.6 Western blot analysis 34
2.2.7 Quantification and statistical analysis 34
2.3 RESULTS 36
2.3.1 hUCB-MSCs ameliorated muscle atrophy 36
2.3.2 Direct or indirect co-culture of hUCB-MSCs alleviate oxidative stress in C2C12 cells 38

2.3.3 hUCB-MSCs regulated iNOS and protein synthesis through AMPK pathway 41
2.3.4 hUCB-MSCs did not modulate mitochondria 43
2.3.5 hUCB-MSCs have a positive effect on motor function and life span of hSOD1-G93A mice 45
2.3.6 The survival intramuscular injected hUCB-MSCs in hSOD1-G93A mice 47
2.3.7 hUCB-MSCs ameliorated oxidative stress and muscle atrophy in the skeletal muscle 49
2.3.8 hUCB-MSCs activated AMPK pathway in the skeletal muscle of hSOD1-G93A mice 53
2.3.9 hUCB-MSCs alleviated degeneration of neuromuscular junctions in the skeletal muscle 55
2.4 DISCUSSION 57

GENERAL CONCOLUSION 60

REFERENCES 62

ABSTRACT IN KOREAN 72

LIST OF ABBREVIATIONS

ALS	Amyotrophic lateral sclerosis
fALS	Familial amyotrophic lateral sclerosis
sALS	Sporadic amyotrophic lateral sclerosis
TARDBP	TAR DNA binding protein
FUS	Fused in sarcoma
C9orf72	Chromosome 9 open reading frame 72
hUCB-MSCs	Human umbilical cord blood mesenchymal stem cells
MuRF1	Muscle RING-finger protein 1
AMPK	AMP-activated protein kinase
MAPK	Mitogen-activated protein kinase
ROS	Reactive oxygen species
RNS	Reactive nitrogen species

CNS	Central nervous system
iNOS	Inducible nitric oxide synthase
NOX2	NADPH oxidase 2
TNF−α	Tumor necrosis factor alpha
IL−1β	Interleukin 1 beta
NMJ	Neuro muscular junction
CAM	Complementary and alternative medicine
tbH_2O_2	tert−butyl hydroperoxide
p70S6K	Ribosomal protein S6 kinase
Mfn1	Mitofusin 1
Mfn2	Mitofusin 2
OPA1	Optic atrophy protein 1
DRP1	Dynamin related protein 1
Bnip3	BCL2/adenovirus E1B 19kDa protein interacting protein 3
HuNu	Human nuclear antigen

CSA	Cross sectional area
TGF-β1	Transforming growth factor beta 1

LIST OF FIGURES

LITERATURE REIVEW

FIGURE 1. ALS disease mechanism and pathology xxi

FIGURE 2. Riluzole and edaravone mechanism xxvi

FIGURE 3. Summary of complementary and alternative medicine xxix

Chapter I

FIGURE 1.1. KCHO-1 attenuated motor impairment and delayed disease onset in hSOD1G93A Tg mice 11

FIGURE 1.2. KCHO-1 attenuated the death of neuronal cells in the spinal cord of hSOD1G93A Tg mice 13

FIGURE 1.3. KCHO-1 attenuated the proliferation and activation of microglial cells..... 16

FIGURE 1.4. KCHO-1 inhibited reactive oxygen species through gp91phox and MAPK..... 19

FIGURE 1.5. KCHO-1 inhibited reactive oxygen species in BV2 microglial cell 22

FIGURE 1.6. KCHO-1 inhibited oxidative stress in BV2 microglial cells via MAPK signaling...

Chapter II

FIGURE 2.1. hUCB-MSCs prevent TGF-β1-induced muscle atrophy 37
FIGURE 2.2. hUCB-MSCs reduced ROS levels induced by TGF-β1 in C2C12 cells 39
FIGURE 2.3. Activation of AMPK by hUCB-MSCs regulated iNOS and protein synthesis in C2C12 cells 42
FIGURE 2.4. Intramuscular transplantation of hUCB-MSCs have positive effects transgenic mice 44
FIGURE 2.5. Intramuscular injection of hUCB-MSCs ameliorated muscle atrophy via inhibition of ROS level in the SOD1 transgenic mice 46
FIGURE 2.6. Intramuscular injected hUCB-MSCs survived at least one week in the skeletal muscle of mice 48
FIGURE 2.7. IhUCB-MSCs reduced the skeletal muscle atrophy through inhibition of

ROS accumulation in the hSOD1−G93A mice 51
FIGURE 2.8. Activation of AMPK regulated protein synthesis and iNOS pathway in the skeletal muscle of hSOD1−G93A mice... 54
FIGURE 2.9. NMJs in the skeletal muscle of each group in hSOD1−G93A mice 56

LIST OF TABLES

TABLE 1. Four marker compounds in KCHO-1 24

LITERATURE REVIEW

Cause of ALS

Amyotrophic lateral sclerosis (ALS) is irremediable disease, which is characterized by death of upper and lower motor neurons (Hardiman et al., 2017). Although the main reason of ALS is largely unknown, many studies have found various genetic causes of ALS and complex factors that cause the pathological features of ALS. Most cases of ALS that are no known cause are called as sporadic ALS (sALS) and these cases are about 90%. The remaining 10% of patients with ALS have a complex familial genetic disorder, and these cases are known as familial ALS (fALS). Among the known gene factors, C9orf72, TARDBP, SOD1 and FUS genes account for up to 70% of all cases of fALS (Huai & Zhang, 2019; Zou et al., 2017).

Mechanism / Pathophysiology

Several genetic research identify the underlying pathogenic mechanism of ALS and suggest molecular mechanism for therapeutic targets (Chia, Chio, & Traynor, 2018). Among them, mutation of SOD1 gene induce neurological pathology including

protein mis-folding, impairment of proteasome pathway, excitotoxicity, oxidative stress, endoplasmic reticulum stress, impaired axonal transport, axonopathy, neuro inflammation, altered RNA processing and mitochondrial dysfunction (Hardiman et al., 2017).

1) Mitochondrial damage and oxidative stress

Mitochondria is an important organelle for several cellular process including cellular respiration, production of energy, and calcium homeostasis (Smith, Shaw, & De Vos, 2019). Disruption of mitochondria has been closely associated with ALS. Especially, abnormal ROS level is directly involved in mitochondria dysfunction of ALS (Smith et al., 2019; Wang, Rayner, Chung, Shi, & Liang, 2020).

Maintaining of low ROS level is important for normal biological functions. However, unbalance between oxidants and antioxidants induce oxidative stress and the unbalance cause the excess level of ROS. Overproduction of ROS can modify or damage to fragmenting of peptide chain, cellular structure, and genetic materials. (Hardiman et al., 2017; G. Kim, Gautier, Tassoni-Tsuchida, Ma, & Gitler, 2020; Tarafdar & Pula, 2018).

The central nervous system (CNS) is especially vulnerable to high level of ROS because of several reasons. First, CNS consume high level of O_2 and produce many ROS and RNS. Second, the major

producer of ROS and RNS are glial cells specifically phagocytic cells indcluding microglia and these stimulated microglial cells express NADPH oxidase. Electron transport chain and NADPH oxidase leak election during biological process and the electron leaking produce superoxide radical (Singh, Kukreti, Saso, & Kukreti, 2019). Overproduction of ROS and RNS are associated with glial activation characterized by astrocytosis, activated microglial cells, and increased expression of iNOS. The abnormalities caused by excessive ROS and RNS are main feature of ALS disease (Islam, 2017).

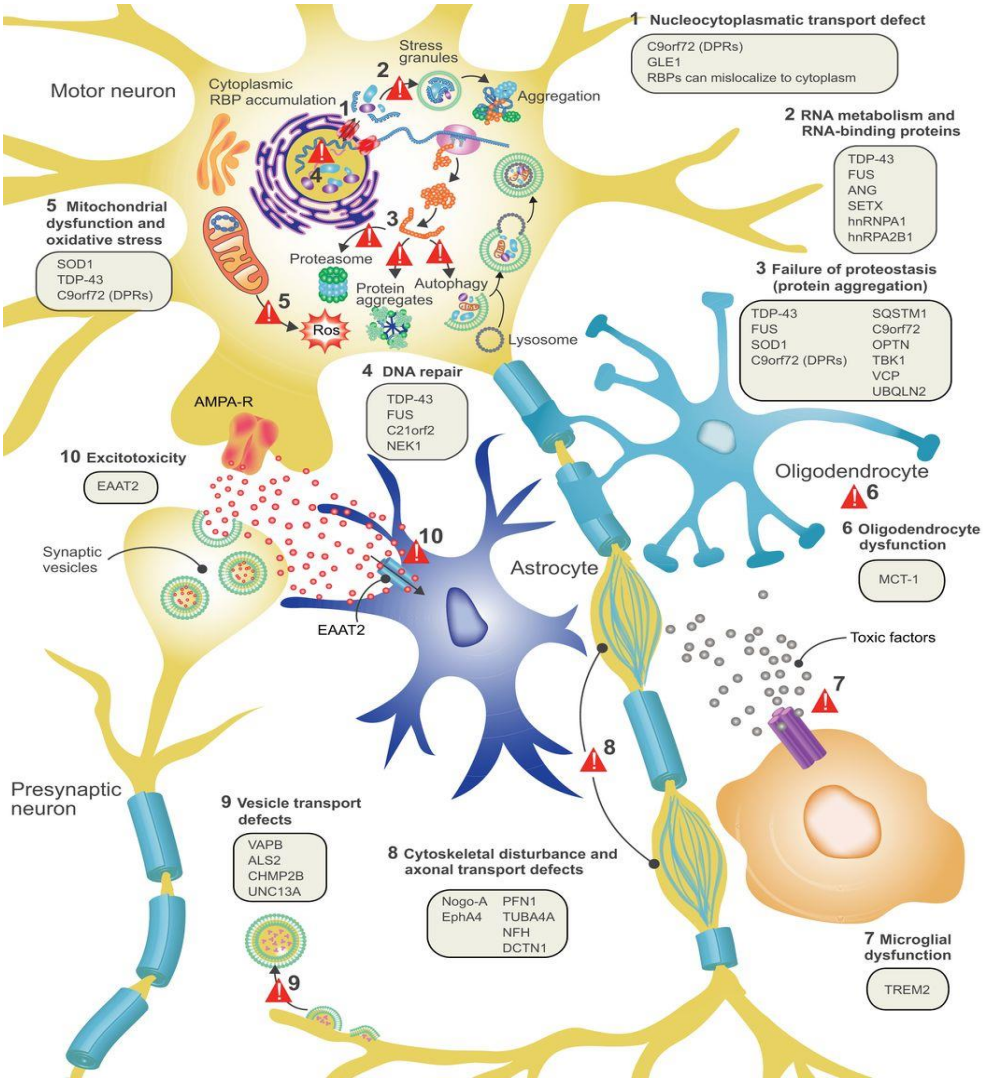

Figure 1. ALS disease mechanism and pathology.

The decline of upper and lower motor neurons is a main character of ALS. Motor neurons are surrounded by microglia, astrocyte and oligodendrocyte.

(Van Damme, Robberecht, & Van Den Bosch, 2017)

2) Activation of microglial cells

In the CNS, glial cells act various function. Among glial cells, microglia cells are considered as brain’s resident immune cells like macrophage and associated with various physiological and pathological features (Ho, 2019). Activation of microglia cells cause polarization of microglia cell in two phenotypes, M1 and M2. The two phenotypes are complex and dynamic mediators of neuronal physiology and induced by several different environmental signals. M1 microglia, which called classical activation, release pro-inflammatory cytokines including TNF-α, IL-1β, prostaglandin E2, ROS and NO (Tang & Le, 2016). In the pathological conditions, M1 microglia produce excessive ROS via NADPH oxidase (NOX2) and mitochondria (Kumar et al., 2016). In contrast, M2 phenotype of microglia cells is neuroprotective type and anti-inflammatory function. Several inflammatory factors like IL-4 or IL-13 stimulate and polarize microglia cells to M2 phenotype. These M2 microglial cells clear cellular debris through phagocytosis. Also, M2 phenotype secrete growth factors and anti-inflammatory cytokines to support neuronal survival (Tang & Le, 2016). As a result, the modulation of M1 or M2 type of microglial cells is a therapeutic option for ALS.

(3) Denervation of neuromuscular junction

Previously accumulated evidence suggest that pathological features of ALS are characterized simultaneously by decline of

motor neurons and skeletal muscle. In the spinal cord, various cells including microglia cells, astrocyte and oligodendrocytes contribute to progression of ALS, and these non-cell-autonomous effects suggest that CNS is a main therapeutic target of ALS (Casas, Manzano, Vaz, Osta, & Brites, 2016; Di Giorgio, Carrasco, Siao, Maniatis, & Eggan, 2007). Beyond the central nervous system, however, skeletal muscle and neuromuscular junction are closely associated with degenerative process. In the neuromuscular junction, the dismantlement of neuromuscular junction proceed along the axon to motor neurons leading to decline of motor neurons and the process is earliest pathology occurring prior to motor neuron death (Lepore, Casola, Dobrowolny, & Musaro, 2019; Tsitkanou, Della Gatta, & Russell, 2016). Although several studies disagree with this, many evidence has been accumulated and demonstrated that malfunction of multiple cell types promote synergistically to proceed the ALS.

(4) The role of AMPK signaling in neuromuscular disease.

AMP-activated protein kinase (AMPK) is a potent mediator of neuromuscular junctions, cellular metabolism, α-motor neurons, and skeletal muscle. Emerging evidences demonstrate that activation of AMPK pathway by pharmacological, genetic or physiological substances alleviate pathologies of neuromuscular disease (Perera & Turner, 2016). Thus, in skeletal muscle, activation of AMPK can

be a therapeutic option for various neuromuscular disease through multiple cellular pathway. Main identification of downstream signaling pathway of AMPK are peroxisome proliferator-activatived receptor γ coactivator 1-α (PGC-1α), ULK1 and CREB. PGC-1α is a master mediator of neuromuscular junction. So, AMPK may maintain and remodel neuromuscular junction through PGC-1α indirectly (Smith et al., 2019). Although the molecular mechanism of the plasticity of neuromuscular junction are needed more research, this result suggest that AMPK also therapeutic target for maintaining of neuromuscular junction. Another study, also, suggest that rescue of AMPK in satellite cells show the regeneration of skeletal muscle and alleviate pathology in the myopathy disease by promoting muscle regeneration (Loeffler, Picchiarelli, Dupuis, & Gonzalez De Aguilar, 2016). Collectively, these results suggest that AMPK signaling can efficiently alleviate neuro-muscular disease and can be a therapeutic target for neuromuscular disease including ALS.

Therapeutic Options for amyotrophic lateral sclerosis

1) Riluzole

Riluzole is a medication approved by FDA for clinical trial to treat ALS. Riluzole, a glutamatergic agent, block the excessive presynaptic release of glutamate from synapse of motor neurons. High level of glutamate at synaptic junction stimulate abnormal signals, which upregulate levels of calcium in post synaptic motor neurons following malfunction and death motor neurons (Cifra et al., 2013; Jaiswal, 2019). As a result, Riluzole show neuroprotection via inhibition of excessive glutamate and voltage-dependent sodium/potassium channels.

2) Edaravone

Edaravone is a novel neuroprotective agent for ALS and is a free radical scavenger. The detailed mechanism of action of Edaravone in ALS is unknown. However, accumulated evidences suggest that Edaravone scavenges hydrogen peroxide and protects neuronal cells against hydrogen peroxide mediated effect via induction of peroxiredoin-2, and inhibition of apoptosis. Under physiological condition, 50% of Edaravone exist as an anion form and Edaravone anion is shown to be an active form for antioxidant (Jaiswal, 2019).

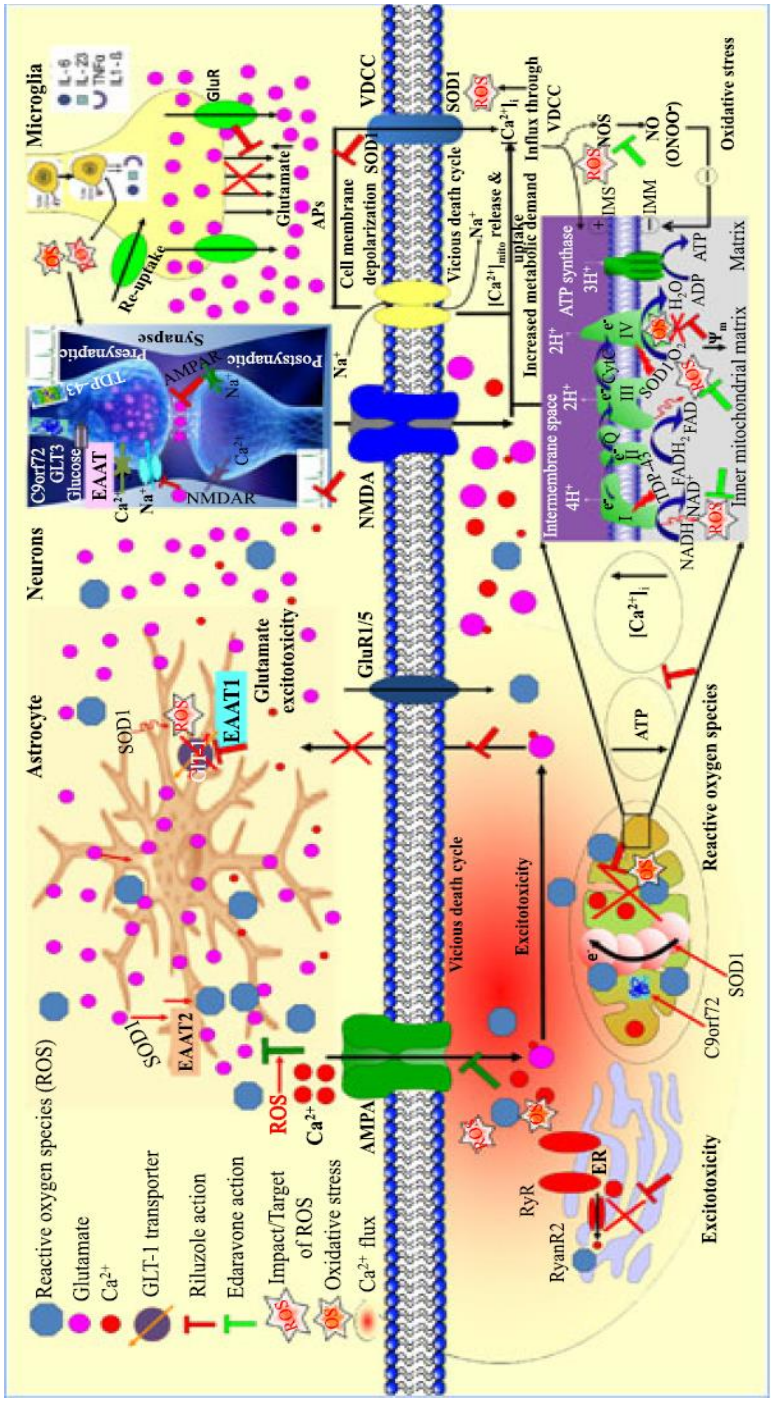

Figure 2. Riluzole and edaravone mechanism.

(Jaiswal, 2019)

Therapeutics

1) Alternative medicine

There are two drugs, Riluzole and Edaravone, approved by FDA for ALS. However, both of the drugs have little effect on ALS patient life by only 2–3 months (Miller et al., 2012). Therefore, there are needs for effective therapy to treat or improve the etiology of ALS. Many previous studies have considered the effectiveness of complementary and alternative medicine (CAM) in ALS animal models and patients to determine the exact mechanism or effect of CAM (Cai, Lee, & Yang, 2019; S. H. Lee & Yang, 2019; Shin et al., 2018; Zhou et al., 2018). Although CAM is a non-mainstream therapy in the field of traditional medicine, the use of CAM, including herbal medicine, has been widely used for a long time in East Asia and recently, many people decided to use of alternative medicine like herbal medicine or acupuncture for the healthcare (Falci, Shi, & Greenlee, 2016; Wasner, Klier, & Borasio, 2001). Especially, herbal medicine like Jaeumganghwa-Tang (JGT) and Gamisoyo-San (GSS), contain various component that have multiple function (S. H. Lee & Yang, 2019; S. Park & Yang, 2018). So it can effect to regulate the pathological feature of ALS including neuro-inflammation, glial activation and oxidative stress. Although these herbal medicines contain various components and can target

multiple pathway, there are little sample size about study to verify the therapeutic effect and mechanism in ALS. So much research needs to be done to confirm the exact therapeutic effect and mechanism of CAM in ALS.

CAM modality	Type of study	Method	Effectiveness
Electroacupuncture (EA)	Animal	Zusanli (ST36) acupoint, (1 mA, 2 Hz, 30 min), 6 times	(Spinal cord) Increased motor activity. neuronal protection, and anti-neuroinflammation
Electroacupuncture (EA)	Animal	Zusanli (ST36) acupoint, (1 mA, 2 Hz, 30 min), 6 times	(Lung) Reduced pro-inflammatory cytokines. and increased cell survival-related protein
Saam acupuncture	Clinical	Taibai (SP3), Taiyuan (LU9), Shaofu (HT8), and Yuji (LU10) twice a day for 5 days	Regulated respiratory physiology
Bee venom (BV)	Animal	0.1 μg/g, Zusanli (ST36), 14 times	(Brainstem and spinal cord) Increased motor activity, survival, anti-inflammation, and neuronal protection
Melittin (MT)	Animal	0.1 μg/g, Zusanli (ST36), 14 times	(Brainstem and spinal cord) Increased motor activity, anti-neuroinflammation, and proteasome activity
Melittin (MT)	Animal	0.1 μg/g, Zusanli (ST36), 14 times	(Lung) Increased anti-inflammation (Spleen) Increased anti-inflammation and cell survival
Scolopendra subspinipes mutilans (SSM)	Animal	2.5 μg/g, Zusanli (ST36), 6 times	(Brainstem and spinal cord) Increased neuronal protection, anti-inflammation, and anti-oxidation
Ginsenoside Re (G-Re)	Animal	2.5 μg/g, Zusanli (ST36), 6 times	(Spinal cord) Increased neuronal protection, anti-inflammation, and anti-oxidation
Withania somnifera	Animal	5 mg/per animal, p.o., 8 or 16 weeks	(Gastrocnemius muscle and spinal cord) Increased motor activity, cognitive function, muscle innervation. Anti-inflammation, anti-NF-kb activation Decreased mislocalization and aggregation of TAR DNA-binding protein 43 (TDP43)
Bojungikgi-tang (BJIGT)	Animal	1 mg/g, p.o., 6 weeks	(Spinal cord and gastrocnemius muscle) Increased motor activity, survival, anti-inflammation, and anti-oxidation Decreased autophagy dysfunction, muscle atrophy, and denervation of neuromuscular junctions
Gamisoyo-San (GSS)	Animal	1 mg/g, p.o., 6 weeks	(Spinal cord) Increased neuronal protection, anti-inflammation, and anti-oxidation Decreased metabolism dysfunction
Gamisoyo-San (GSS)	Animal	1 mg/g, p.o., 6 weeks	(Gastrocnemius muscle) Increased anti-inflammation and anti-oxidation
Jaeumganghwa-Tang (JGT)	Animal	1 mg/g, p.o., 6 weeks	(Spinal cord) Increased motor function, anti-inflammation, and anti-oxidation
Huolingshengji Formula (HLSJ)	Animal	4.5 g/kg·d, p.o., 100 days	(Spinal cord, Gastrocnemius muscle) Increased motor activity and survival, anti-apoptotsis and anti-inflammation, Decreased muscle atrophy
Huolingshengji Formula (HLSJ)	Clinical	200 ml, p.o., 12 weeks	Decreased Advanced Norris scale score (ANSS) Improved TCM syndrome
Dihuang Yinzi (DHYZ)	Clinical	Decoction, p.o., twice daily, 12 years	Increased survival, muscle fibrillation, and muscle strength Delayed use of ventilator support Fewer adverse effects
Jiawei Sijunzi (JWSJZ)	Clinical	Decoctions, p.o., 50 ml, twice daily	Improved neurological evaluation according to the ALS functional rating scale (ALSFRS)
Creatine	Animal	2% creatine-fed, 4 weeks	Improved motor performance, weight maintenance, and survival
Creatine	Animal	2% creatine-fed, 60 days	No effect on muscle metabolic parameters, muscle weight, muscle contractile parameters, and fatigability
Creatine	Clinical	doses ranging from 5 – 10 g per day	No effect on survival and ALS functional rating revised scores (ALSFRS-R) progression or percent predicted forced vital capacity (FVC) progression
Vitamin D	Clinical	2000 IU/day, 9 months, daily	Decreased revised ALS functional rating scale (ALSFRS-R) score
Vitamin E	Animal	200 IU/kg of mouse chow, Treatment continued until end-stage disease	Delayed disease onset and slow progression

Figure 3. Summary of complementary and alternative medicine

(Cai & Yang, 2019)

2) Stem cell therapy

Various stem cell therapies are one of the therapeutic option for ALS therapy. Many clinical trials have identified the effects and mechanisms of various stem cells in patients with ALS. The advantage of stem cells is that they secrete trophic factors that provide supportive milieu and may replace damaged cells with new ones (Baloh et al., 2018; Mazzini et al., 2003). In some cases, it has been demonstrated that transplanted stem cells survive long term and differentiate into damaged neuronal cells. However, there is no lasting improvement due to unsuitable connections between neurons and transplanted stem cells (Mazzini et al., 2003; Sahni & Kessler, 2010).

These results demonstrated that although stem cell transplantation can replace neurons with new neurons, proof of concept for effective connections between neurons is needed. Thus, alternative strategies of transplantation of stem cells are to modulate nearby cells by providing immunomodulation, trophic factors, and supports other neuronal cells such as glial cells and oligodendrocytes that interact with motor neurons (Chen, Kankel, Su, Han, & Ofengeim, 2018). Furthermore, Mesenchymal stem cells (MSCs) can secret various factors including immune-modulators, chemokine and neurotrophic factors that could support neuronal survival and alleviate neurodegeneration (Ciervo, Ning, Jun, Shaw, & Mead, 2017; Mazzini et al., 2003).

Chapter 1

A novel herbal compound, KCHO-1, reduced reactive oxygen species in the spinal cord of amyotrophic lateral sclerosis

1.1 Introduction

Amyotrophic lateral sclerosis, also known as Lou Gehrig' s disease, is a progressive and fatal disease characterized by the death of upper and lower motor neurons in the central nervous system (CNS). During disease progression, a decrease in lower motor neurons leads to muscle atrophy, while upper motor neuron degeneration induces spasticity (Mejzini et al., 2019). The main pathology of ALS is still unknown, but accumulated evidence suggests several pathological mechanisms such as protein mis-folding, protein aggregation, oxidative stress and glutamate excitotoxicity (Hardiman et al., 2017). There are two form of ALS. Sporadic ALS (sALS) is the majority of ALS cases, with about 5-10% of cases considered familial ALS (fALS). Up to the present, previous studies have identified more than 30 distinct genes related with fALS, especially mutations in the SOD1 gene, which have been studied most extensively (Huai & Zhang, 2019). The mutant SOD1 cause the neurodegenerative feature like oxidative stress, neuro-inflammation and activation of glial cells (Bordt & Polster, 2014). Previous study have found that excessive ROS cause motor neuron death and other pathological features (Bordt & Polster, 2014; Bozzo, Mirra, & Carri, 2016). Among the pathological features, stimulation

of microglial cells induce oxidative stress during the progress of neurodegeneration in the CNS of ALS (Boillee & Cleveland, 2008). Especially, activated microglial cells expressed gp91phox, which is known as NOX2, and produce high level of ROS under ALS condition (Hooten, Beers, Zhao, & Appel, 2015; Liao, Zhao, Beers, Henkel, & Appel, 2012; Zhao, Beers, & Appel, 2013). The excessive increase of ROS by inducing the expression of gp91phox in the microglial cells induce pathological signals that produce neurotoxic factors through MAPK pathway and inhibition of the expression of gp91phox alleviated disease progression of ALS mouse model (E. K. Kim & Choi, 2010; Marden et al., 2007; Wu, Re, Nagai, Ischiropoulos, & Przedborski, 2006). Up to date, several therapeutic options have been carried out but there are no significant effect (Bucchia et al., 2015; Palomo & Manfredi, 2015; Yang et al., 2010). The novel compound, KCHO-1, is extracted and organized by traditional herbal compounds that are *Curcuma longa, Salvia miltiorrhiza, Gastrodia elata, Chaenomeles sinensis, Polygala tenuifolia, Paeonia japonica, Glycyrrhiza uralensis, Atractylodes japonica* and processed *Aconitum carmichaeli*. The combination of these nine herbs has been widely used in the place of conventional medicine (Jeong et al., 2014; D. S. Lee et al., 2014).

Taken together, we found and demonstrate that KCHO-1 inhibit production of ROS and prevent decline of motor neurons and activation of microglial cells in an SOD1 transgenic mice through

NOX2 inhibition. As a result, administration of KCHO-1 improved lifespan of ALS mouse model via gp91phox and MAPK signaling pathway and KHCO-1 can be a therapeutic option for ALS.

1.2 MATERIALS AND METHODS

1.2.1 Animals

The hSOD1G93A transgenic mice are hemizygous transgenic B6SJL mice carrying the mutant human SOD1 gene with a glycine to alanine base pair mutation at the 93rd codon of the cytosolic Cu/Zn superoxide dismutase (B6SJL-Tg(SOD1*G93A)1Gur/J). The transgenic mice were purchased from the Jackson Laboratory (Bar Harbor, ME, USA). For sorting the transgenic mice, genomic DNA was extracted and a we performed PCR assay. All mice were housed at a constant temperature of 21-23℃ and a humidity of 50-60% with a 12-hour light/dark cycle. All animal experiments were performed according to the guidelines of the Laboratory Animals Resources institute (SNU-120821-5-1, Seoul National University, Republic of Korea).

1.2.2 Materials

KCHO-1 is a compound of herbs, which are Curcuma longa, Salvia miltiorrhiza, Gastrodia elata, Chaenomeles sinensis, Polygala tenuifolia, Paeonia japonica, Glycyrrhiza uralensis, Atractylodes japonicam and processed Aconitum carmichaeli. KCHO-1 was

processed and deposited at the Hanpoong Pharm & Foods Co., Ltd. (K-GMP). The criteria for selection of marker compounds were based on the quantitative method of the Korean Pharmacopeia (TABLE 1) (Jeong et al., 2014; D. S. Lee et al., 2014).

1.2.3 Motor function analysis

Before rotarod test was performed, the mice underwent training time before the test to adapt to the apparatus (7650 Accelerating model, Ugo Basile Biological Research Apparatus, Comerio, Italy). The motor function was evaluated as the time the tested mice could withstand the rotarod test at a rotational speed of 10 rpm. Testing was conducted every other day.

1.2.4 MTT assay

The BV2 microglial cells were cultured in Dulbecco's modified Eagle's medium (Gibco, USA; 11995) with 10% FBS (Gibco, USA; 16000), 1% penicillin and streptomycin (Gibco, USA; 15140). The MTT solution (5mg/ml, Sigma, USA) incubated for 4h. Absorbance was measured at a wavelength of 540 nm in the supernatant using an EL800 microplate reader (Bio-Tek, USA)

1.2.5 Nitric oxide and ROS assay

The ROS level of the tissue was measured by using H_2DCFDA.

The tissues were incubated with 5μM H_2DCFDA (ThermoFisher, USA; D399). The nitrite oxide concentration was measured using the colorimetric Griess Reagent (Promega, USA; TB229) according to the manufacturer's instructions. The CellROX oxidative stress reagents (Life Technologies, USA; C10422) was used for 30 min at 37℃ to measure ROS levels.

1.2.6 Western blotting

The protein of tissues was extracted with a protein extraction kit (pro-prep, iNtRON Biotechnology Inc., Seoul, Republic of Korea). The protein in each sample was quantified with the Bio-Rad DC protein assay kit (Bio-Rad Laboratories, Foster City, CA, USA). For western blotting, protein samples were electrophoresed on a 10-12% SDS-polyacrylamide gel and transferred to a nitrocellulose membranes. The blots were blocked with 5% BSA in TBST for 1 hour and then incubated with various primary antibodies including beta-Actin (sc-47778), GADPH (cell signaling #2118S), anti-Iba1 (wako 019-19741), anti-GFAP (ab7260), anti-iNOS (ab15323), anti-gp91phox (ab80508). Blots were incubated with appropriate secondary antibodies (1:1000; Invitrogen) and then developed with chemiluminescence reagents (Amersham Pharmacia, Piscataway, NJ, USA). All western blot data were performed with the ImageJ v1.48 software (National Institutes of Health, USA)

1.2.7 Immunohistochemistry

The spinal cord (L2-L4) was dissected out, fixed in 4% PFA following incubation with 30% sucrose. The embedding was performed with OCT compound (Sakura Finetek, Japan). The section was blocked with 3% NGS in PBS following incubation of the primary antibody including anti-Iba1 and anti-GFAP. After that, the sections were incubated with the appropriate secondary antibodies (1:2000; Molecular Probes, Eugene, OR, USA), followed by 4',6-Diamidino-2-phenylindole dihydrochloride (DAPI; Santa Cruz Biotechnology Inc., Santa Cruz, California, USA). All data were analyzed with an Eclipse TE200 confocal microscope (Nikon, Japan).

1.2.8 Histology

For Fluoro-jade C staining (FJC staining) the tissues were immersed in 100% and 70% alcohol for 3 min. Thereafter, the tissues were transferred with 0.06% potassium permanganate (KMnO4) for 15 min, washed with dH2O and then stained with the 0.001% Fluoro-Jade staining solution for 30 min. Detection of Nissl bodies was performed by Nissl staining. Briefly, Sections were incubated in 1:1 alcohol/chloroform, immersed in 100% and 95% alcohol and dH2O for rehydration. After that, the tissues were incubated with 0.1% cresyl violet (Sigma-Aldrich, Germany). For

H&E staining, the tissues were stained with H&E using standard protocols. All histological data was performed by using an Eclipse TE200 confocal microscope (Nikon, Japan).

1.2.9 Statistical analysis

Data were presented as mean ± SEM and analyzed with Graphpad (GraphPad Software, CA, USA). The results of immunoblotting data between the KCHO-1 and vehicle group were compared via t-test. The mean ages ± s. d. of statistical analyses of the SOD1 transgenic mice is presented graphically using an unpaired t-test for comparison between each group, and a log-lank test was used for the Kaplan-Meier survival analysis.

1.3 RESULTS

1.3.1 KCHO-1 attenuated motor impairment and delayed disease obset in hSOD1G83A Tg mice

Total experiment scheme was figure out briefly (Fig. 1.1a). During the rotarod test, the onset of the disease was determined when tested mice first fell out of the apparatus and found that administration of KCHO-1 (127.8 ± 3.1) delayed the onset of disease compared to treatment in the vehicle (118.9 ± 1.1) group (Figure 1.1b).

The rotarod test suggested that administration of KCHO-1 improved motor function, while the motor function of the vehicle-group rapidly decreased. Especially, there was significant difference in the rotarod score from day 114 to 130 (Figure 1.1c).

To determine the lifespan, the Kaplan-Meier survival test was used. The KCHO-1 group survived longer than the vehicle group. The average lifespan of the KCHO-1 group was 139 days, and the vehicle group was 128 days (Figure 1.1d, e). These results demonstrate that oral administration of KCHO-1 can alleviate disease progression and improve survival in SOD1 transgenic mice.

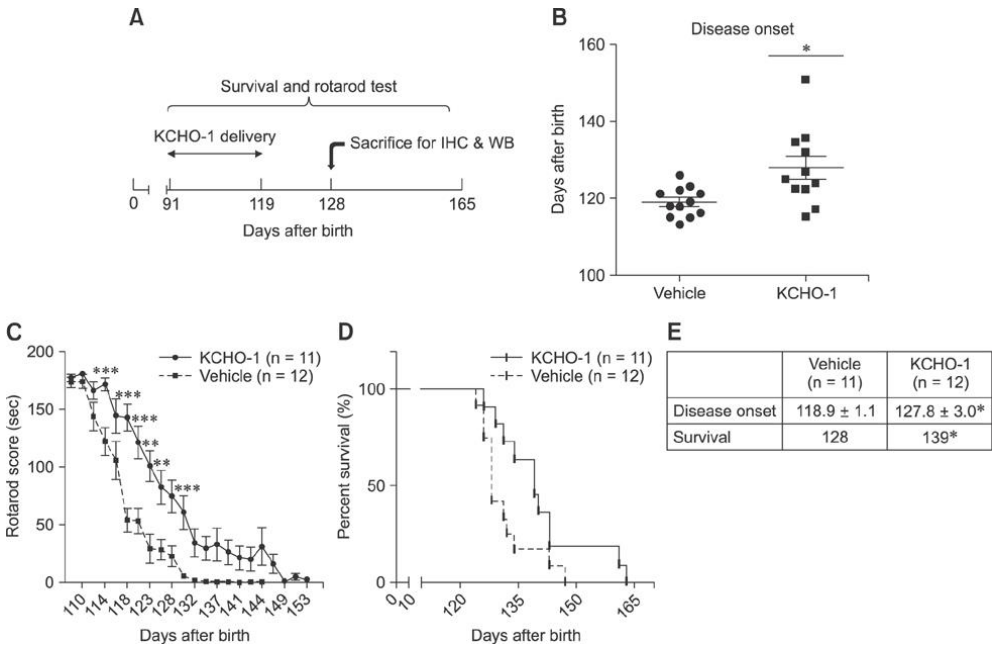

Figure 1.1 KCHO-1 attenuated motor impairment and delayed disease onset of ALS mice model

(A) Each group were separated into two group and delivered KCHO-1(250mg/Kg/day) or normal saline. (B) The day of disease onset was improved by KCHO-1 (127.8 ± 3.1) compared with vehicle group (118.9 ± 1.1). (C) Administration of KCHO-1 significantly improved motor function between day 114 and 130. (D) KCHO-1 improved survival rate of the SOD1 transgenic mice. The average lifespan of the KCHO-1 group was 139 days, and the vehicle group was 128 days. (E) Summary of statistical significance of differences in disease onset and survival. $*p < 0.05$, $**p < 0.01$, $***p < 0.001$.

1.3.2 KCHO-1 attenuated the death of neuronal cells in the spinal cord of hSOD1G93A Tg mice

To identify if KCHO-1 ameliorate neuronal death in the spinal cord of SOD1 transgenic mice, we examined histological examination of the lumbar spinal cord in KCHO-1- and vehicle-treated mice. H&E staining of the spinal cord suggested that there were more nerve cell bodies in the KCHO-1 group than in the vehicle-treated group (Figure. 1.2a). Furthermore, Nissl staining was performed to confirm the Nissl bodies in neurons and found that the number of neuronal cells in vehicle- and KCHO-1 mice were 5.9 ± 0.6 and 11.7 ± 0.6, respectively (Figure. 1.2b, d). Furthermore, FJC staining of the spinal cord suggested that the number of degenerative neurons was significantly reduced from 41.5 ± 2.8 in the vehicle group to 31.2 ± 1.7 in the KCHO-1 group (Figure. 1.2c, e).

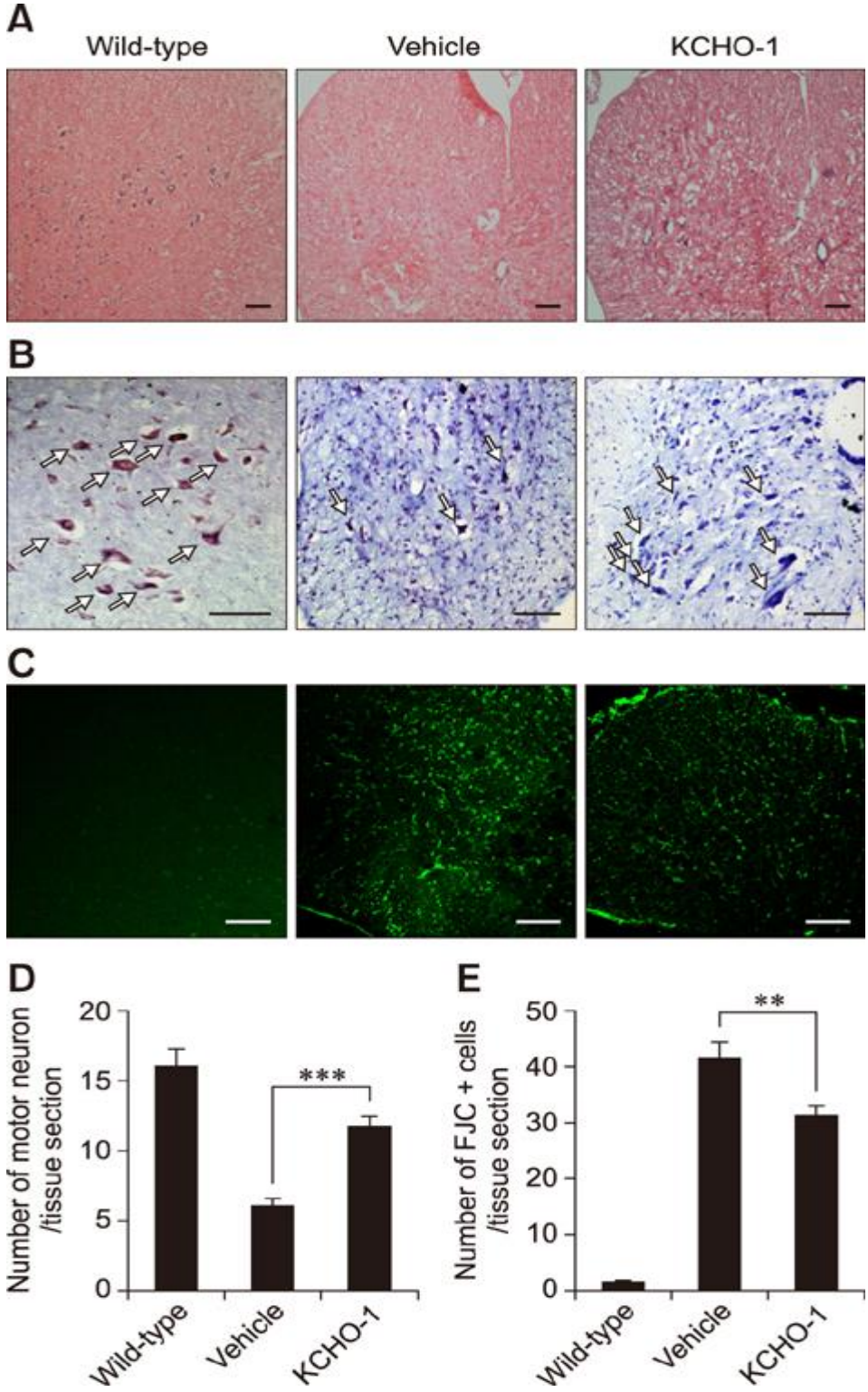
A
Wild-type
Vehicle
KCHO-1
B
C
D
Number of motor neuron /tissue section
20
15
10
5
0
***
Wild-type
Vehicle
KCHO-1
E
Number of FJC + cells /tissue section
50
40
30
20
10
0
**
Wild-type
Vehicle
KCHO-1

Figure 1.2. Oral administration of KCHO-1 improved neuronal survival in the spinal cord of ALS mouse model.

(A, B) H&E and Nissl staining in the anterior horn of spinal cord of each group showed that neuronal cells survived more in the KCHO-1 group than in the vehicle group (C) In the spinal cord of each group FJC-positive cells (green) that showed degenerative neurons were significantly reduced in the KCHO-1 group (D) When counting nissl bodies larger than a certain size, the number of motor neurons was significantly higher in the KCHO-1 gorup(11.7 ± 0.6) than the vehicle group (5.9 ± 0.6). (E) The number of FJC positive neurons was ameliorated in KCHO-1 group (31.2 ± 1.7) compare to vehicle group (41.5 ± 2.8). Scale bar represents 100μm; magnification is 100× or 200×. Data were presented as mean ± SEM values (n = 3-4 per group) and analyzed by one-way ANOVA. $*p < 0.05$, $**p < 0.01$, $***p < 0.001$.

1.3.3 KCHO-1 attenuated the proliferation and activation of microglial cells

To determine whether KCHO-1 ameliorated or inhibited activation of glial cells including microglia and astrocyte, we measured the expression of Iba1 and GFAP that are marker of glial cells (Figure 1.3A). The fluorescence intensity of Iba-1 decreased in the KCHO-1 group (Vehicle: 12.32 ± 0.39, KCHO-1: 11.05 ± 0.36), but there was not significant difference between the groups in GFAP intensity (Vehicle: 11.05 ± 0.57, KCHO-1: 11.39 ± 0.34) (Figure 1.3B).

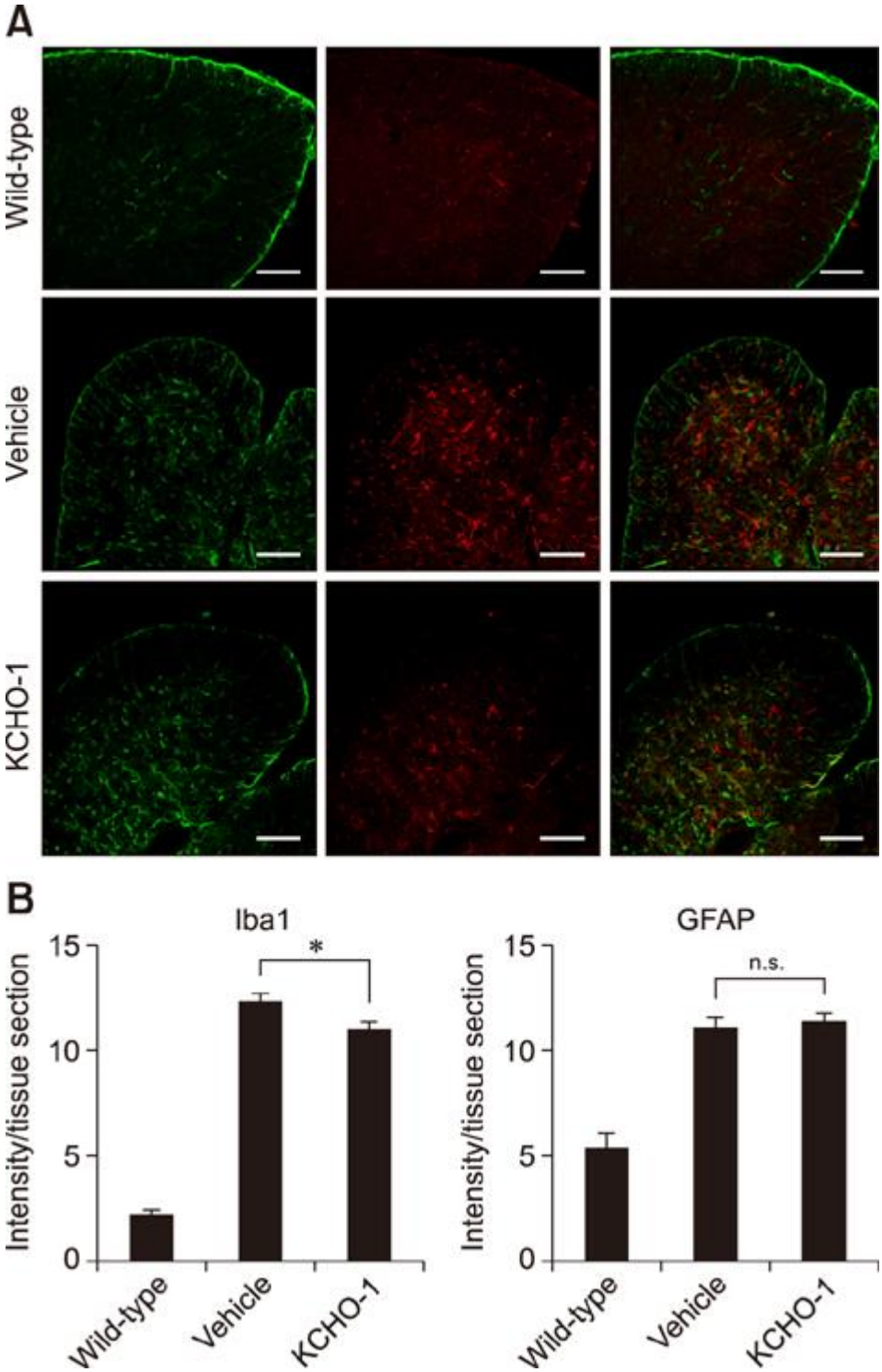
A
Wild-type
Vehicle
KCHO-1
B
Iba1
Intensity/tissue section
15
10
5
0
*
Wild-type
Vehicle
KCHO-1
GFAP
Intensity/tissue section
15
10
5
0
n.s.
Wild-type
Vehicle
KCHO-1

Fig. 3. Oral administration of KCHO-1 ameliorated microglial cell activation in the spinal cord of SOD1 transgenic mice.

(A) Representative immunohistochemical images of each group showed expression of Iba1-positive microglia (red) and GFAP-positive astrocyte (green) in the spinal cord of each group. (B) Compared to the vehicle group, KCHO-1 suppressed the fluorescence intensity of Iba1, but the fluorescence intensity of GFAP was not significantly different between the groups. Scale bar represents 100 μm; Data were presented as mean ± SEM values and analyzed using one-way ANOVA (n = 3-4 per group). $*p < 0.05$

1.3.4 KCHO-1 inhibited oxidative stress through gp91^{phox} and MAPK

We investigated whether KCHO-1 regulates oxidative stress via gp91^{phox} and the MAPK pathway in SOD1 transgenic mice. First, we found that administration of KCHO-1 reduced ROS levels in the spinal cord of SOD1 transgenic mice (Figure 1.4A). Next, we examined whether inducible NOS (iNOS) and NADPH oxidase (gp91^{phox}) protein levels were modulated by KCHO-1 and found that iNOS (WT: 0.1 ± 0.01, vehicle: 0.48 ± 0.04, KCHO-1: 0.25 ± 0.1) and gp91^{phox} (WT: 0.23±0.12, vehicle: 2.02±0.24, KCHO-1: 1.08 ± 0.13) protein level was decreased in the KCHO-1 group (Figure 1.4B,C). To confirm Whether KCHO-1 regulated the MAPK pathway at the protein level, we investigated protein level in ERK1/2 and p38. The phosphorylated ERK1 (WT: 0.28 ± 0.07, vehicle: 2.72 ± 0.21, KCHO-1: 1.66 ± 0.31) and ERK2 (WT: 0.11, vehicle: 2.06 ± 0.05, KCHO-1: 1.19 ± 0.14) were reduced in the KCHO-1 group, but the phosphorylated p38 (WT: 0.28 ± 0.16, vehicle: 1.72 ± 0.11, KCHO-1: 1.19 ± 0.23), was not significantly different in each group (Figure 1.4D, E).

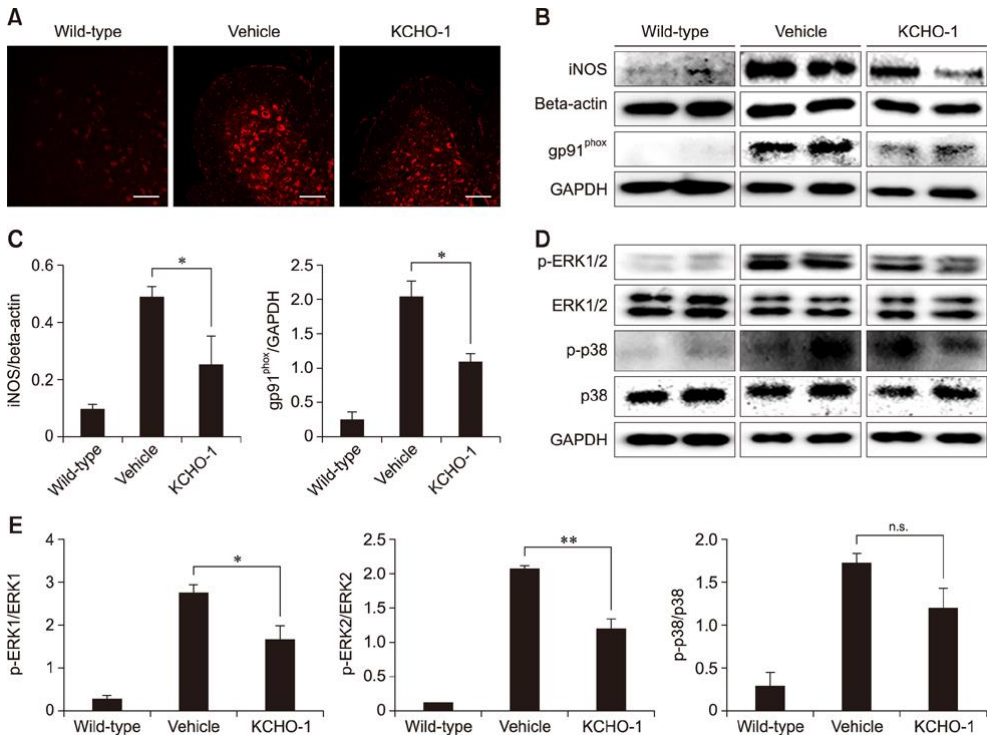

Figure 1.4. KCHO-1 inhibited reactive oxygen species through gp91^{phox} and MAPK.

(A) KCHO-1 reduced the level of ROS in the spinal cord compared to the vehicle group. (B, C) Protein level of iNOS and gp91^{phox} were decreased in the KCHO-1 group compared to the vehicle group. (D, E) Protein level of ERK1/2 and p38 MAPK pathway was investigated. The pERK1/2 protein level was decreased in the KCHO-1 group than in the vehicle group. There was no significant difference in the pp38 protein level. The data were presented as mean ± SEM values and analyzed using one-way ANOVA (n = 3-4 per group). $*p < 0.05$, $**p < 0.01$

1.3.5 KCHO-1 inhibited reactive oxygen species in BV2 microglial cells

To verify the effect of KCHO-1 on activated microglial cells, BV2 microglial cells were stimulated by IFNγ and LPS with varying concentrations of KCHO-1. In activated microglial cells, ROS levels significantly increased (48.98 ± 3.8) compared to negative control (5.84 ± 0.7), whereas KCHO-1 significantly reduced ROS level at 50 and 100μg/mL (36.74 ± 1.7 and 37.61 ± 1.2, respectively) (Figure 1.5A, B). The cytotoxicity of KCHO-1 was investigated through MTT assay on BV2 cells at various concentrations (Figure 1.5C). In addition, we evaluated NO_2^- and ROS levels in BV2 microglial cells. Activated microglial cells increased the secretion of NO_2^- (17.35 ± 1.27) whereas KCHO-1 treatment attenuated NO_2^- production at 50μg/mL (12.17 ± 1.65) and 100μg/mL (10.65 ± 0.97) (Figure 1.5D).

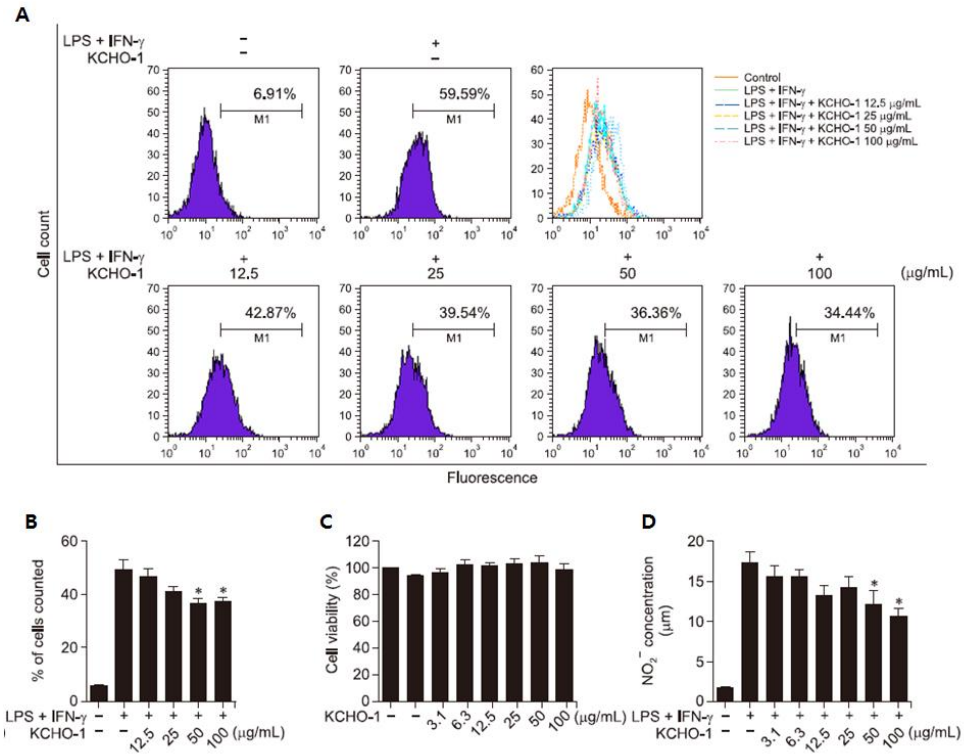

Figure 1.5. KCHO-1 reduced oxidative stress by inhibiting ROS in BV2 microglial cells

(A) FACS analysis of activated BV2 cells treated with various concentration of KCHO-1 before staining with cellROX. (B) At 50 and 100μg/mL concentration, KCHO-1 significantly reduced ROS levels in activated BV2 cells. (C) The cytotoxicity of KCHO-1 against BV2 microglial cells was evaluated by MTT assay. There was no significant toxicity to the cells up to 100μg/ml. (D) Griess assay was performed on activated BV2 cells to measure NO levels, and KCHO-1 significantly reduced NO level at 50 and 100μg/ml concentrations.

1.3.6 KCHO-1 inhibited oxidative stress in BV2 microglial cells via MAPK signaling

At the protein level, KCHO-1 reduced iNOS and the $gp91^{phox}$ level in stimulated BV2 microglia. In particular, 100μg/mL of KCHO-1 dramatically reduced iNOS (0.65 ± 0.12) and $gp91^{phox}$ (0.6 ± 0.11) level (iNOS: 1.17 ± 0.09, $gp91^{phox}$: 1.32 ± 0.19) (Figure 1.6A). Previous study have shown that intracellular ROS activates the MAPK pathway and *vice versa* (Apolloni et al., 2013). So we investigated the MAPK pathway including p38 and ERK1/2. The p-p38 (1.41 ± 0.24) and pERK1/2 (ERK1: 1.64 ± 0.24, ERK2: 1.33 ± 0.14) protein levels were increased in the stimulated group compared to the control group (p38: 0.07 ± 0.07, ERK2: 0.15 ± 0.15). specifically, 100μg/ml of KCHO-1 significantly reduced p38 (0.4 ± 0.18) and ERK1 (0.43 ± 0.16) phosphorylation in stimulated cells. The same concentration of KCHO-1 also reduced the expression of pERK2 (0.74 ± 0.04), but the reduction was not significant (Figure. 1.6B).

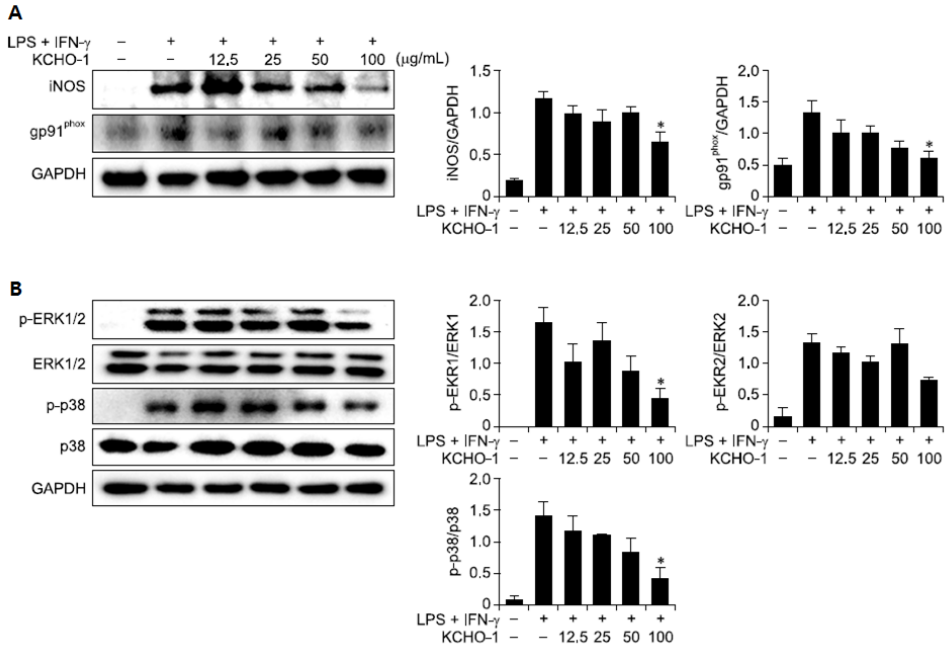

Figure 1.6. KCHO−1 inhibited oxidative stress and MAPK pathway in BV2 microglial cells.

(A) Western blot analysis of the effects of various concentrations of KCHO−1 in activated BV2 cells. KCHO−1 inhibited the expression of iNOS and gp91^{phox} protein. In particular, 100μg/mL KCHO−1 significantly reduced the expression of iNOS and gp91^{phox} proteins. (B) At 100μg/mL concentration, KCHO−1 significantly reduced the expression of pERK1, but did not significantly decrease the expression of pERK2 and p−p38. Density measurements from western blots were normalized to GAPDH or total form values. Data were presented as mean ± SEM values from three independent experiments. $*p < 0.05$ compared with the LPS + IFNγ (+) KCHO−1 (−) group.

Table 1.1 Four marker compounds of KCHO-1

Name	Curcumin	Glycyrrhizic acid	Paeoniflorin	Salvianolic acid B
Chemical formula	$C_{21}H_{20}O_6$	$C_{42}H_{62}O_{16}$	$C_{23}H_{28}O_{11}$	$C_{36}H_{30}O_{16}$
Molar mass	368.38	822.93	480.46	718.62

1.4 DISCUSSION

Many previous studies have investigated the effect and mechanism of complementary and alternative medicine (CAM). Especially, previous study found that *G. elata, A. japonica* and *S. miltiorrhiza have effect on neuroprotection or* anti-inflammation. *C. longa, C. sinensis,* and *P. tenuifolia* have antioxidant activity, Furthermore, *G. uralensis and P. japonica have* antibacterial function and *A. carmichaeli* can reduce pain (Du et al., 2013; J. A. Hong et al., 2003; M. H. Hong et al., 2010; W. Y. Jiang et al., 2013; B. W. Kim et al., 2012; K. S. Kim et al., 2013; Y. Kim et al., 2014; Manavalan et al., 2012; Sancheti, Sancheti, & Seo, 2013; Villinski et al., 2014; Xu et al., 2006). These traditional medicines have been accepted for a long time and used for the cure of many diseases. Previous studies suggested that several concentrations of KCHO-1 relieve inflammation through inhibition of NF-kB pathway and ROS via HO-1 in microglial cells (D. S. Lee et al., 2016) (D. S. Lee et al., 2014). In this study, we found that oral administration of KCHO-1 improved motor activity and lifespan in SOD1 transgenic mice and reduced neuronal loss through inhibition of ROS. Furthermore, we found that KCHO-1 inhibited activation of microglial cells but not astrocytes. The microglial cells are macrophage cells of the CNS

and chronic stimulation of microglial cells produce ROS that cause the pathological features of ALS (Kobayashi et al., 2013; Zhang & Jiang, 2015).

Previous studies have shown that the mutant SOD1 protein stimulated microglial cells and increased ROS production through NADPH oxidase (Barber & Shaw, 2010; Boillee & Cleveland, 2008; Wu et al., 2006). Furthermore, when microglial cells expressed simultaneously NADPH oxidase with iNOS, these microglial cells produce various neurotoxic factors and ROS following neuronal death (Brown & Neher, 2010; Mungrue, Husain, & Stewart, 2002; Takeuchi et al., 1998). Based on this results, we found that the expression levels of $gp91^{phox}$ and iNOS protein increased in SOD1 transgenic mice, and administration of KCHO-1 reduced oxidative stress in SOD1 transgenic mice with decreased expression of $gp91^{phox}$ and iNOS protein. Furthermore, oxidative stress induced by $gp91^{phox}$ activated the MAPK pathway and increased a stress signaling pathway in the CNS of ALS (Apolloni et al., 2013). In this study, we found that KCHO-1 inhibited the activation of microglial cells through inhibition of $gp91^{phox}$ and iNOS. Likewise, oral administration of KCHO-1 in SOD1 transgenic mice reduced the activation of the ERK1/2 pathway but did not significantly decrease p38 activation. In SOD1 transgenic mice, mutant SOD1 proteins, inflammatory cytokines, and ROS are able to activate the p38-MAPK pathway in astrocytes. In this study, KCHO-1 had no

functional effect on p38, and these results may have been associated with the lack of a significant effect on astrocytes (Ben Haim, Carrillo-de Sauvage, Ceyzeriat, & Escartin, 2015; E. K. Kim & Choi, 2010). Therefore, it is necessary to explain the link between the p38-MAPK pathway and the effect of KCHO-1 on ALS.

In this study, we demonstrated that KCHO-1 inhibited oxidative stress through $gp91^{phox}$ and the MAPK pathway in activated microglial cells. Moreover, we showed that the administration of KCHO-1 has a therapeutic effect on $hSOD1^{G93A}$ transgenic mice. Thus, KCHO-1 could be a therapeutic option for ALS treatment.

Chapter Ⅱ

hUCB-MSCs transplanted into skeletal muscle improved motor function and survival of the SOD1 G93A mice by activating AMPK

2.1 INTRODUCTION

Amyotrophic lateral sclerosis is a fatal neurodegenerative disease that lead to the motor neuron and muscle degeneration. Although previous studies found several pathophysiological mechanism of ALS including glutamate excitotoxicity, mitochondrial dysfunction and oxidative stress, the main causes of ALS disease are not yet investigated(Geloso et al., 2017; J. Jiang & Ravits, 2019; Weishaupt, Hyman, & Dikic, 2016). The Riluzole and Edaravone, a glutamatergic neurotransmission inhibitor and ROS scavenger, are approved for cure of ALS but they have limited effects on disease progression and survival (Jaiswal, 2019; Lunn, Sakowski, & Feldman, 2014). Furthermore, under the disease progression, the skeletal muscle is critically affected during disease progression (Xiao et al., 2018). In the ALS, the interaction of various cells that is known non-cell autonomous was associated with disease progress. Consistent with this idea, several studies have shown that the disease pathology observed first in patients is degeneration of NMJ in skeletal muscle. The "dying-back" hypothesis, which specifies the degeneration of neuromuscular junctions occurs before the death of motor neuron, has shown the importance of skeletal muscle in ALS progression (Di Pietro et al., 2017; Dupuis

et al., 2009; Fischer et al., 2004). In this regard, muscle atrophy and neuromuscular degeneration, along with the death of motor neuron in ALS, play an important role in ALS. However, the skeletal muscles involved in the death of motor neurons have not been fully identified, and methods of improving the pathology of ALS through skeletal muscle have not been well studied to date.

Although the mechanisms leading to pathological features of ALS have not been fully identified, several studies have suggested potential mechanisms including AMPK signaling (Lim et al., 2012; Liu, Ju, et al., 2015; Liu, Lee, Lai, & Chern, 2015; Perera et al., 2014). However, there are controversial results about the effect of AMPK activity for ALS treatment. Latrepirdine and Resveratrol, activators of AMPK signaling, improve survival rate and delay disease progression on SOD1 transgenic mice (Coughlan, Mitchem, Hogg, & Prehn, 2015; Mancuso et al., 2014). In addition, another study found that synaptic dysfunction in the outer retina was remodeled through AMPK activation (Dial, Ng, Manta, & Ljubicic, 2018; Samuel et al., 2014). In contrast, Metformin, an activator of AMPK signaling, promotes disease pathology in ALS (Kaneb, Sharp, Rahmani-Kondori, & Wells, 2011). Although previous studies have suggested various therapeutic options for ALS, there is no effective treatment for ALS. However, stem cell therapy is proposed as a promising option for the treatment of neurodegenerative disease (Gugliandolo, Bramanti, & Mazzon, 2019; Rehorova et al., 2019).

Recent clinical trials have confirmed that hMSC transplantation in patients with ALS is safe and has a beneficial effect on the patient. (Gugliandolo et al., 2019; Oh et al., 2018; Petrou et al., 2016; Rehorova et al., 2019; Sykova et al., 2017).

The purpose of the study here was to confirm the therapeutic effect of repeated intramuscular administration of hUCB-MSCs in the SOD1 transgenic mouse model. Previous studies have shown that administration of hMSC through skeletal muscle is effective in inducing positive effects in SOD1 transgenic mice (Gugliandolo et al., 2019; Rehorova et al., 2019), but the mechanism of hUCB-MSCs on skeletal muscle in ALS disease is not fully understand. Thus, we demonstrated the positive effects and therapeutic mechanisms of hUCB-MSCs in relation to muscle atrophy and regulation of the AMPK pathway in ALS.

2.2 MATERIALS AND METHODS

2.2.1 Animals.

The hSOD1 G93A transgenic mice (B6.Cg-Tg(SOD1*G93A)1Gur/J) used in this study were purchased from Jackson Laboratories (USA). Animals in this study were handled by the guidelines of the Laboratory Animals Resources Institute (SNU-141124-1, Seoul National University, Korea). All mice tested were housed in individual cages under constant environmental conditions (21 - 23℃ temperature, 50-60% humidity and 12h light/dark cycle). For each individual experiment, same age and only female mice were used.

2.2.2 Rotarod and disease onset

Body weight and motor function was investigated for measuring the disease progression. All mice tested were trained for a week and rotarod tests were performed three times a week using a rotarod apparatus (Ugo Basile, Italy). Rotarod accelerates at 10rpm over 3min and mice were tested three times per test.

2.2.3 Cell culture

C2C12 cells were purchased from ATCC. C2C12 myoblast were

seeded in dish with DMEM high with 10% FBS to 80-90% confluency. At that time, the media was changed to DMEM high with 1% HS to differentiate myoblast to myotube for 7days. The C2C12 myoblast cells were plated and differentiated for one week in DM. After differentiation to myotube, N-acetyl cysteine were pretreated in myotube for 2hrs and 10ng/ml TGF beta1 were treated in myotube and incubated for 24hrs. After incubation, it was washed with PBS, and hUCB-MSCs were cultured on the transwell insert for 24hrs.

2.2.4 Immunocyto- and Immunohistochemistry

To quantifying the diameter of myotubes in several groups, immunostaining was performed on differentiated myotube. The permeabilization was performed with 1% triton X-100 and blocked with 5% NGS. Myotubes were incubated with 1:1000 MF20 (DSHB) antibody overnight at 4℃, 1:1000 secondary antibody (Thermo) was incubated for 1h and DAPI for 10min. For diameter quantification, 20 myotubes per images were randomly selected.

The isolated gastrocnemius was frozen in liquid nitrogen-chilled isopentane and cryoembedded with an OCT compound (Tissue Tek, Germany) for frozen sections. Cryo-samples were cut to 10 μm thickness. Sections were stained like immunocytochemistry.

2.2.5 ROS assay.

ROS levels were determined using 2,7-dichlorofluorescein diacetate (H2-DCFDA, thermo). H2-DCFDA was treated in each group of myoblasts for 20min following PBS washing. After staining, cells were trypsinized and centrifuged. After that, the cells were collected in PBS and measured by flow cytometry (BD Bioscience, USA). For ROS staining of skeletal muscle, cryo-samples were incubated with 2,7-dichlorofluorescein diacetate at 37℃ for 30min.

2.2.6 Western blot analysis

Western blotting was performed and blotted onto a nitrocellulose membrane. For blocking, the membrane was incubated with 5% BSA for 1h and probed with appropriated antibodies including p-AMPK, AMPK, iNOS, p-p70s6k, p70s6k, p62, LC3 1/2, p-AKT, AKT and GAPDH. After that, the appropriate HRP conjugated secondary antibodies were probed in the membrane.

2.2.7 Quantification and statistical analysis

All statistical analyzes were performed in GraphPad Prisms software. For quantification, one-way ANOVA was used to investigate the significance between three or more groups. *$p<0.05$; **$p<0.01$; ***$p<0.001$; ns, no significance. Result are reported mean ± SEM. The Kaplan-Meier method was used to determine

survival rates. All data are presented as the mean ± standard error of the mean (SEM).

2.3 RESULTS

2.3.1 hUCB-MSCs ameliorated muscle atrophy in C2C12 cells

It is well known that TGF-β1 regulates the pathological condition characterized by muscle atrophy and previous studies have suggested that mesenchymal stem cell-conditioned media inhibit oxidative stress and muscle atrophy in C2C12 cells (Abrigo, Simon, Cabrera, & Cabello-Verrugio, 2016; C. M. Park et al., 2016). In this study, we co-cultued hUCB-MSCs with C2C12 myotubes stimulated by TGF-β1 for 24hrs and confirmed differences in muscle atrophy in each group. We found that TGF-β1 increased the number of low-width C2C12 cell myotubes compared to the negative control (0-10㎛; TGF-β1: 8.14, Control: 5.13, 10-15㎛ TGF-β1: 23.0, Control: 16.3) and hUCB-MSCs improved the reduction in the number of high-width C2C12 myotubes compared to the TGF-β1 treated group ($P<0.05$, 15-20㎛ TGF-β1: 6.14, hUCB-MSCs: 11.7, 20-30㎛ TGF-β1: 2.71, hUCB-MSCs: 8.00). Although the mRNA level of MuRF1 was not affected, the mRNA level of MAFbx/atrogin1 was observed to decrease significantly in the hUCB-MSCs group ($P<0.05$, Figure 2.1C).

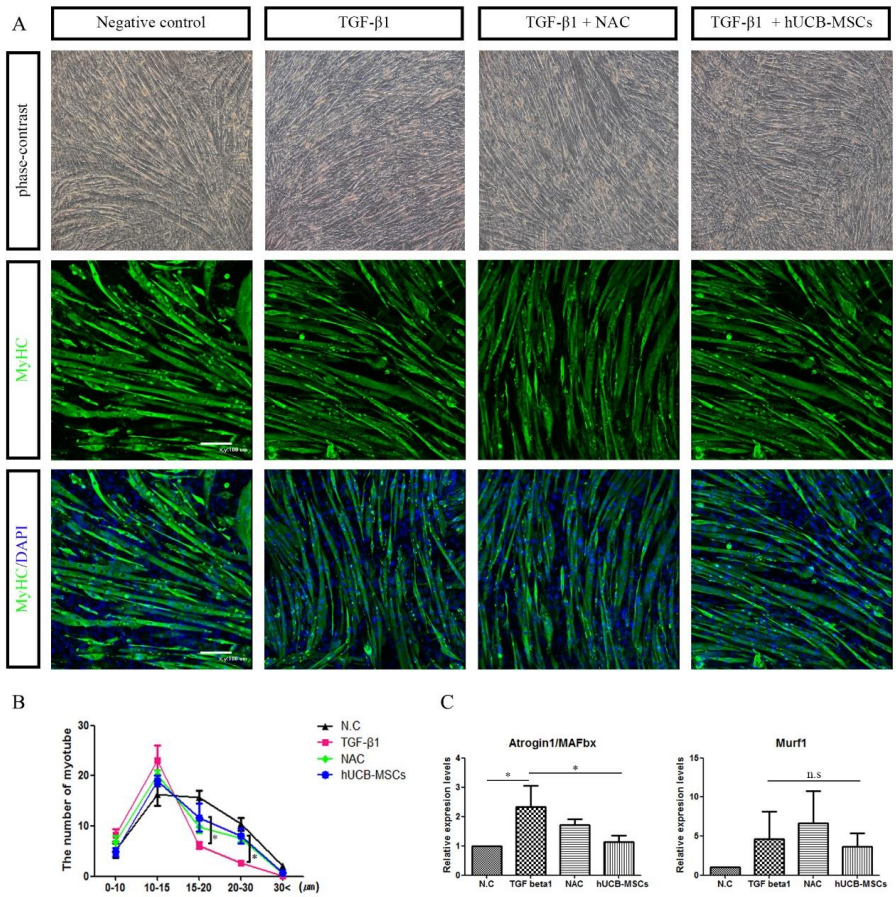

Figure 2.1. hUCB-MSCs prevented muscle atrophy in C2C12 cells.

(A) Representative images of C2C12 myotube incubated with or without TGF-β1 and hUCB-MSCs. (B) The number of C2C12 myotube for each width in each group was plotted. TGF-β1 vs hUCB-MSCs. *P<0.05. (C) The mRNA level of MAFbx/atrogin1 and Murf1 was measured. All data were analyzed by one-way analysis. *P<0.05, n.s: not significant.

2.3.2 Direct or indirect co-culture of hUCB-MSCs alleviate oxidative stress in C2C12 cells

Previous study suggested that hUCB-MSCs inhibit oxidative stress caused by tbH2O2 in C2C12 cells (Abrigo, Rivera, Simon, Cabrera, & Cabello-Verrugio, 2016). To verify that muscle atrophy is regulated by ROS in C2C12 cells, we evaluated whether co-culture of hUCB-MSCs inhibited ROS level in C2C12 cells, and we found that the mRNA expression of MAFbx/atrogin1, not MuRF1, was significantly reduced in the hUCB-MSC group compared to the tbH2O2 group ($P<0.05$, Figure 2.2C, D).

Next, we investigated whether hUCB-MSCs protected C2C12 cells from muscle atrophy by inhibiting intracellular ROS levels. As a result, we found that direct co-culture of hUCB-MSCs reduced ROS levels in C2C12 cells (Figure 2.2A). In addition, indirect co-culture of hUCB-MSCs was performed to confirm whether hUCB-MSCs were able to indirectly regulate ROS level induced by TGF-β1. Again, hUCB-MSCs could inhibit ROS level induced by TGF-β1 in C2C12 cells (Figure 2.2B).

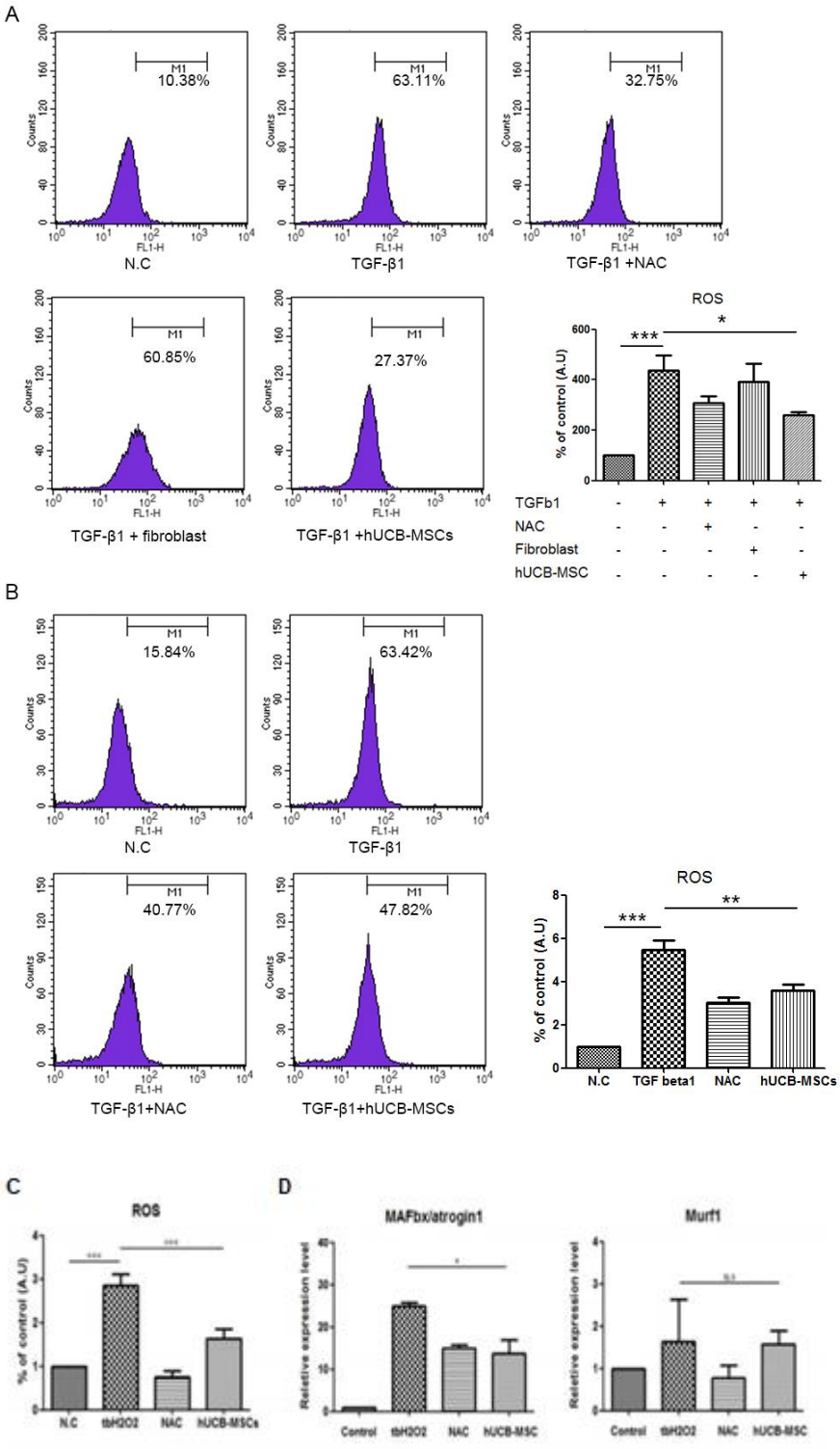
A
M1
10.38%
N.C
63.11%
TGF-β1
32.75%
TGF-β1 +NAC
60.85%
TGF-β1 + fibroblast
27.37%
TGF-β1 +hUCB-MSCs
ROS
% of control (A.U)
TGFb1
NAC
Fibroblast
hUCB-MSC
B
15.84%
N.C
63.42%
TGF-β1
40.77%
TGF-β1+NAC
47.82%
TGF-β1+hUCB-MSCs
ROS
% of control (A.U)
N.C
TGF beta1
NAC
hUCB-MSCs
C
ROS
% of control (A.U)
N.C
tbH2O2
NAC
hUCB-MSCs
D
MAFbx/atrogin1
Murf1
Relative expression level
Control
tbH2O2
NAC
hUCB-MSC

Figure 2.2. hUCB-MSCs inhibited oxidative stress caused by TGF-β1 in C2C12 cells.

TGF-β1 effectively induced ROS in C2C12 cells, and the resulting ROS was measured by H2-DCFDA and FACS analysis. (A) C2C12 cells were co-cultured directly with hUCB-MSCs with or without TGF-β1 and ROS levels were measured. In the NAC group, C2C12 cells were treated with NAC for 2hrs prior to TGF-β1 treatment. (B) To confirm the indirect effect of hUCB-MSCs, TGF-β1-treated C2C12 cells were co-cultured with or without hUCB-MSCs and ROS levels were measured. (C, D) hUCB-MSCs reduced ROS induced by tbH2O2, and mRNA levels of muscle atrophy markers were suppressed by hUCB-MSCs. Graphs were presented as a percentage of the negative control and analyzed by one-way analysis. *P<0.05, **P<0.01, ***P<0.001

2.3.3 hUCB-MSCs regulated iNOS and protein synthesis through AMPK pathway.

Intracellular ROS regulate mitochondrial biogenesis in various cells through SIRT1/AMPK/PGC1-α pathway (Bak et al., 2019). To investigate whether the hUCB-MSCs regulate intracellular ROS through promotion of mitochondrial dysfunction, we assessed the AMPK pathway in myotubes. Although TGF-β1 alone did not modulate AMPK protein level in myotubes, hUCB-MSCs activated the AMPK protein in myotubes (Figure 2.3A). Furthermore, mRNA level of SIRT1 and PGC1-α were increased in the hUCB-MSC group, but the mRNA level of PGC1-α was not significantly different (Figure 2.3D). In order to investigate other components that associated with muscle atrophy, we investigated iNOS and protein synthesis in C2C12 myotubes. Each line of hUCB-MSCs decreased the expression of the iNOS protein, which is consistent with a decrease in NO level co-cultured with hUCB-MSCs indirectly (Fig 3A and C). We also evaluated the protein level of ribosomal protein S6 kinase (p70S6K). TGF-β1 reduced the phosphorylation of the p70S6K (p-p70S6K) protein level and both hUCB-MSCs prevented a decrease in the p-p70S6K protein level. (Figure 2.3A, B).

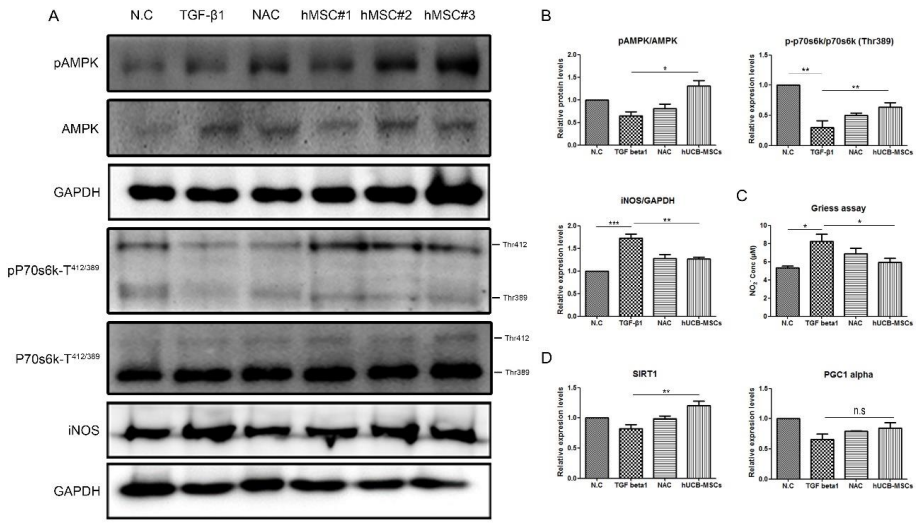

Figure 2.3. Activation of AMPK induced by hUCB-MSCs inhibited the expression of iNOS and protein synthesis in C2C12 myotubes.

(A) C2C12 myotubes were treated with TGF-β1 in co-cultured with or without hUCB-MSCs. Co-cultured hUCB-MSCs inhibited the expression of iNOS and increased the expression of p-p70S6K protein in C2C12 myotubes. (B) Quantification and relative expression level of each band of western blot are shown in the graph. (C) The level of NO concentration in C2C12 myotubes was indicated for each group. (D) The mRNA expression level of SIRT1 and PGC1-α was indicated for each group. All signals were visualized by ECL detection. All data were represented as mean ± SEM for three independent experiments and analyzed by one-way analysis. *P<0.05, **P<0.01, ***P<0.001

2.3.4 hUCB-MSCs did not modulate mitochondrial dynamics in myotubes

Mitochondrial Malfunction is closely related with ALS disease. So we investigated mRNA level of the mitochondrial dynamics-related genes mitofusin1 (Mfn1), mitofusin2 (Mfn2), optic atrophy protein1 (OPA1), dynamin-related protein1 (DRP1) and BCL2/adenovirus E1B 19 kDa protein-interacting protein 3 (Bnip3). However, there were no significant differences between each group (Figure 2.4).

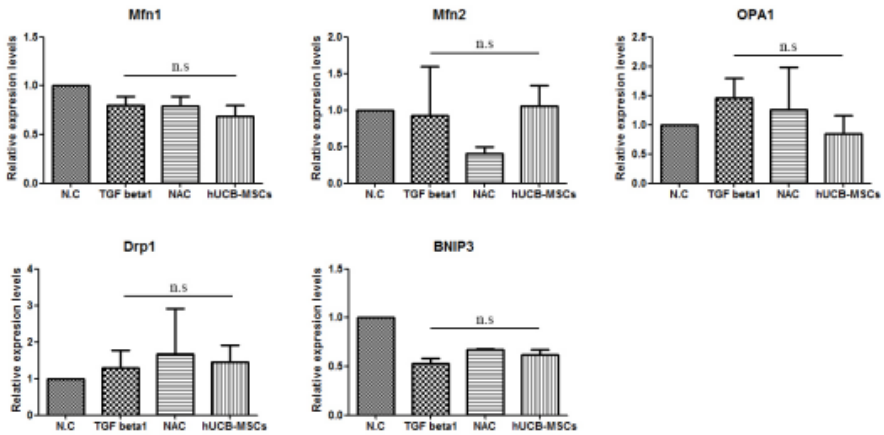

Figure 2.4. Mitochondrial related genes did not altered by hUCB-MSCs

(A) Effect of co-culture of hUCB-MSCs on the mRNA level of mitochondrial related genes in C2C12 myotubes. The mRNA expression level of mitochondrial related genes was not changed in C2C12 myotubes by hUCB-MSCs and TGF-β1.

2.3.5 hUCB-MSCs positively affected motor function and increased longevity in hSOD1-G93A mice.

In hSOD1-G93A mice, a motor function study with rotarod test was performed to confirm the potential of hUCB-MSCs for therapeutics. Rotarod was tested every other day and transplanted hUCB-MSCs improved motor activity in SOD1 transgenic mice from days 108 to 119 (Figure 2.4A). In addition, body weight was improved in the hUCB-MSCs group and there was a significant difference between days 119 to 126 (Figure 2.4B). The disease onset of hSOD1-G93A mice based on body weight was improved in the hUCB-MSC group (mean 131.7 ± 2.86, $p<0.05$) compared to the control group (mean 121.7 ± 3.363) (Figure 2.4C).

The survival rate of hUCB-MSC transplanted animals ($p<0.05$, mean 144.0 days) was improved compared to the control group (mean 127.5 days) (Figure 2.4D, E). Overall, these results suggested that repeatedly applied hUCB-MSCs improved motor function and extended lifespan in hSOD1-G93A mice.

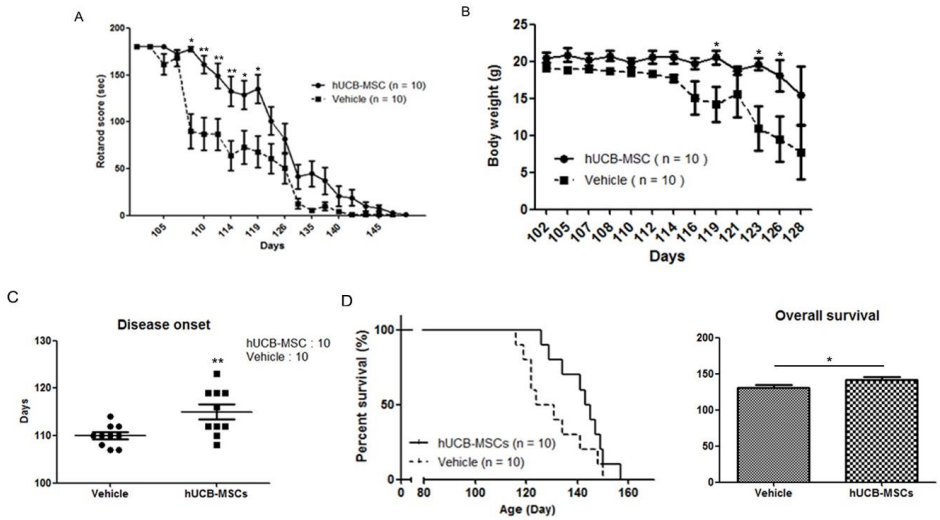

Figure 2.5. Intramuscular administration of hUCB-MSCs improved motor activity and survival rate in hSOD1-G93A mice.

(A) Intramuscular administration of hUCB-MSCs showed improvement in the rotarod score. (B) hUCB-MSCs effectively delayed weight loss in SOD1 transgenic mice compared to the control. (C) The onset of disease was delayed in the hUCB-MSCs group compared to the vehicle group. (D) hUCB-MSCs increased the survival rate of SOD1 transgenic mice when compared to the control. *P<0.05, **P<0.01, t-test for rotarod and disease onset, log-rank test for survival curves.

2.3.6 The survival intramuscular injected hUCB-MSCs in hSOD1-G93A mice

We should investigate whether the intramuscular transplantation of hUCB-MSCs were survived at least for 1 weeks because we transplanted hUCB-MSCs once a week. For investigation of the survival of hUCB-MSCs in skeletal muscle, we implanted GFP-tagged hUCB-MSCs. A week later, we stained the tissues with a human-specific marker for nuclei (HuNu) and found GFP-tagged hUCB-MSCs co-localized with HuNu. These results show that intramuscularly implanted hUCB-MSCs survived for at least 1 week between muscle fibers (Figure 2.5A).

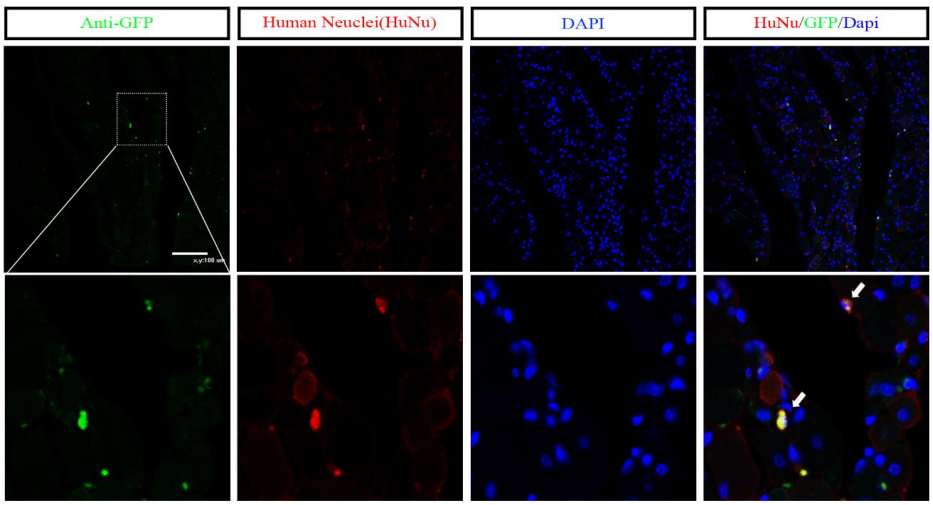

Figure 2.6. Intramuscular injected hUCB-MSCs survived at least one week in the skeletal muscle of mice.

For investigating survival of hUCB-MSCs, GFP tagged hUCB-MSCs were used. Representative imuunohistochemical images of GFP and Human Nuclei in the gastrocnemius muscle. One week after transplantation of hUCB-MSCs in the gastrocnemius muscle, human specific marker for nuclei and anti-GFP expression were detected and GFP expression was co-localized with the expression of HuNu in the tissue.

2.3.7 hUCB-MSCs ameliorated oxidative stress and muscle atrophy in skeletal muscle of hSOD1-G93A mice.

We investigate whether hUCB-MSCs also alleviated the skeletal muscle atrophy in the SOD1 transgenic mice (Figure 2.7A). To compare each group, we investigate cross sectional area (CSA) of the gastrocnemius muscle in each groups. Most of the CSA analysis of gastrocnemius in mice ranged from 100 to 1200 μm, but in the gastrocnemius muscle of wild type CSA, it was distributed from 300 to 3000 μm. The application of hUCB-MSCs significantly increased the fiber ratio from 500 to 700 μm compared to control group ($p<0.05$, Figure 2.7C). On the other hand, the proportion of small fibers (100 to 300 μm^2) was higher in the vehicle group than in the hUCB-MSC group, but the difference was not significant. Similar to the fiber ratio, the mean of total CSA was higher in the hUCB-MSC group ($p<0.05$, 685.2 ± 13.21) than in the vehicle group (615.6 ± 14.41, Figure 2.7C). In the cumulative percentage distribution of CSA, there was a left shift in the CSA distribution in the vehicle (649.477 ± 15.531) and hUCB-MSCs (685.211 ± 13.21) groups compared to wild type (1066.49±26.8882). hUCB-MSCs treated fibers also shifted to the right down to the 1000 μm^2 fiber size compared to the control group ($P<0.001$, Figure 2.7D).

We also observed a high accumulation of ROS levels in skeletal

muscle (Figure 2.7B) and measured the intensity of DHE expression in skeletal muscle in each group and found a significant decrease in ROS level in hUCB-MSCs (17.86 ± 1.201) compared to vehicle group (24.32±1.529) ($P<0.001$, Figure 2.7E).

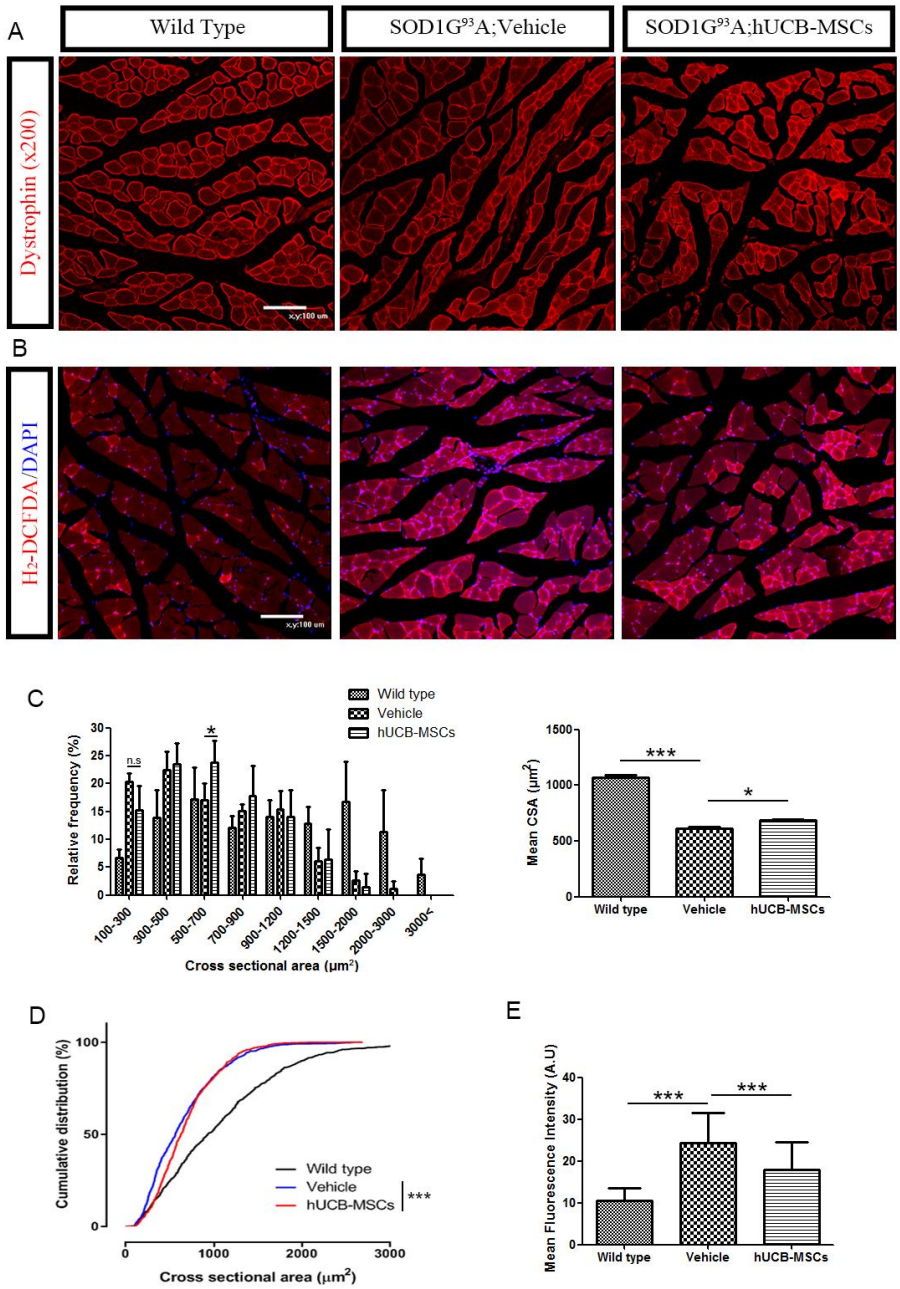
A
Wild Type
SOD1G93A;Vehicle
SOD1G93A;hUCB-MSCs
Dystrophin (x200)
B
H2-DCFDA/DAPI
C
Wild type
Vehicle
hUCB-MSCs
Relative frequency (%)
n.s
*
100-300
300-500
500-700
700-900
900-1200
1200-1500
1500-2000
2000-3000
3000<
Cross sectional area (μm2)
Mean CSA (μm2)
***
*
Wild type
Vehicle
hUCB-MSCs
D
Cumulative distribution (%)
Wild type
Vehicle
hUCB-MSCs
***
Cross sectional area (μm2)
E
Mean Fluorescence Intensity (A.U)
***
***
Wild type
Vehicle
hUCB-MSCs

Figure 2.7. hUCB-MSCs reduced skeletal muscle atrophy through inhibition of ROS accumulation in hSOD1-G93A mice.

Skeletal muscle morphology and ROS levels in each group. (A) Representative immunohistochemical images of dystrophin for comparing CSA in each group. (B) DHE analysis to assess ROS levels in gastrocnemius muscle in each group. Representative images of three group of mouse tissues (n = 3) (C) Frequency distribution of CSA in skeletal muscle in each group (n = 3). (D) Cumulative percentage distribution of total CSA in skeletal muscle in each group. (E) The intensity of ROS in skeletal muscle in each group. The differences in each group were analyzed by one-way ANOVA and the cumulative percentage distribution was analyzed by Kolmogorov-Smirnov test. *P<0.05, **P<0.01, ***P<0.001

2.3.8 hUCB-MSCs activated the AMPK pathway in skeletal muscle of hSOD1-G93A mice.

To verify whether intramuscular injection of hUCB-MSCs could regulate the expression of iNOS and p70S6K in hSOD1-G93A mice through AMPK pathway, we performed western blot and found that hUCB-MSCs transplanted to skeletal muscle increased expression of AMPK ($P<0.05$, Figure 2.8A, C). Furthermore, the hUCB-MSC group increased the phosphorylated expression of AKT and p70S6K proteins in skeletal muscle of SOD1 transgenic mice compared to the vehicle group ($P<0.05$, Figure 2.8B, C). In addition, hUCB-MSCs significantly inhibited the expression of the iNOS protein ($P<0.05$, Figure 2.8B, C). These results demonstrated that hUCB-MSCs can rescue protein synthesis and inhibit iNOS expression in skeletal muscle of transgenic mice.

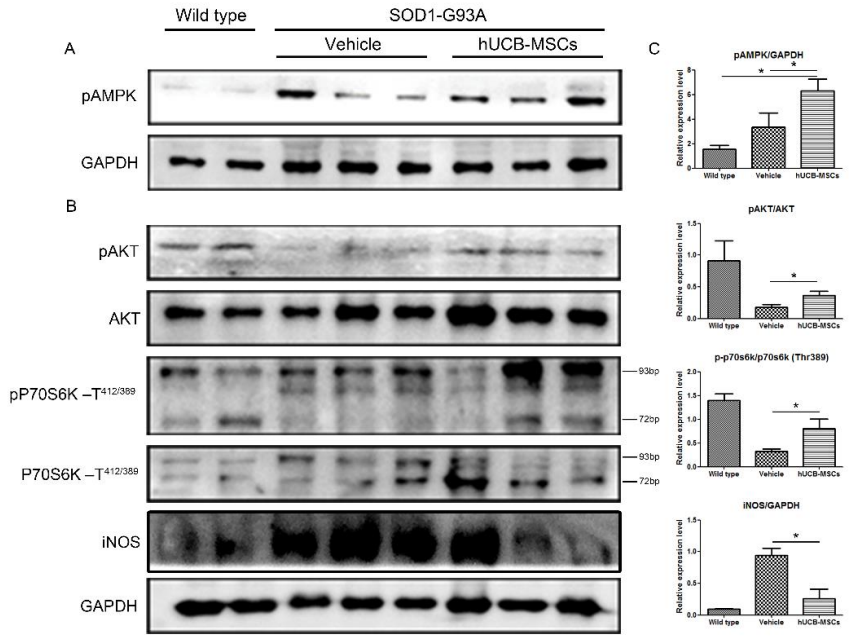

Figure 2.8. Activation of AMPK by hUCB-MSCs rescued protein synthesis and inhibited iNOS in skeletal muscles of hSOD1-G93A mice.

(A) Western blot showing the levels of phosphorylated AMPK in skeletal muscle of WT and ALS mouse model with or without hUCB-MSCs. Skeletal muscle transplanted with hUCB-MSCs showed increased expression of p-AMPK protein. (B) hUCB-MSCs increased the expression of p-AKT and p-P70S6K proteins and decreased the expression of iNOS protein in skeletal muscle of each group. (C) Statistical analysis of p-AMPK, p-AKT, p-P70S6K and iNOS (n = 2 ~ 3). *P<0.05, one-way ANOVA.

2.3.9 hUCB-MSCs alleviated the degeneration of neuromuscular junctions in the skeletal muscle of hSOD1-G93A mice.

The expression of ROS and AMPK was closely related to the mediation of the neuromuscular junction (NMJ) (Dial et al., 2018; Pollari, Goldsteins, Bart, Koistinaho, & Giniatullin, 2014). In line with this, we investigated the degeneration of NMJs and found that hUCB-MSCs alleviated denervation in the skeletal muscles of SOD1 transgenic mice (Figure 2.9A). To investigate the morphology of the NMJs, the morphology was classified into one of three types: pretzel, perforated, and disorganized. In the skeletal muscle of each group, the skeletal muscle of WT had a higher level of pretzel form than the SOD1 transgenic mice group, and more pretzel forms were detected in the hUCB-MSCs group than in the vehicle group. Administration of hUCB-MSC reduced the proportion of disorganized NMJs compared to vehicle group, but the difference was not significant (Figure 2.9B). However, hUCB-MSCs (387.7 ± 23.47, $p<0.05$) rescued the endplate area when compared to the vehicle group (304.7 ± 14.24, Figure 2.9C). These results suggested that repeated intramuscular transplantation of hUCB-MSCs improved NMJ degeneration in hSOD1-G93A mice.

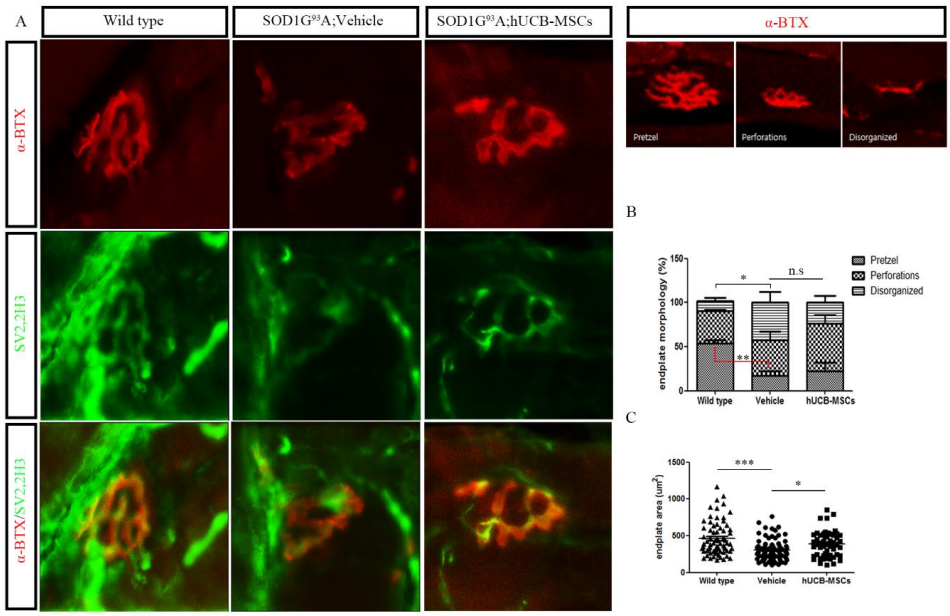

Figure 2.9. NMJs in skeletal muscle of each group in hSOD1-G93A mice.

Reduced NMJ morphology in skeletal muscle of the ALS mouse model. (A) Images of the post-synaptic end plates and presynaptic nerve terminals showed denervation and structure of NMJs in each group. (n = 3) (B) The morphology of the endplate has been classified into three types: Pretzel, Perforated and Disorganized. There was no significant difference between the vehicle and the hUCB-MSCs group. (C) Measurement of NMJ end plate area of skeletal muscle in SOD1 transgenic mice. All data shown were means ± SEM and analyzed by one way ANOVA. *P<0.05, **P<0.01, ***P<0.001.

2.4 DISCUSSION

MSCs have been considered potential therapeutics for many diseases as they have been shown to have several properties, including regulation of inflammatory conditions, release of cytokines and growth factors that promote various signaling pathway. In particular, in clinical trials, MSCs have been used as treatment option for patients (Gugliandolo et al., 2019) (Ichim et al., 2010; C. M. Park et al., 2016; Suzuki et al., 2008). Many studies to date have found that transplantation of MSCs into the CNS, skeletal muscle or both has a positive effect on survival rate and motor activity in the ALS mouse model (Forostyak et al., 2014; Oh et al., 2018; Rehorova et al., 2019). In this study, we found that hUCB-MSCs had a positive effect on skeletal muscle of SOD1 transgenic mice. However, how hUCB-MSCs protect skeletal muscle of SOD1 transgenic mice is not fully understood. To understand mechanism by which hUCB-MSCs prevent pathology of skeletal muscle during disease progression, we have repeatedly implanted hUCB-MSCs into the skeletal muscle of SOD1 transgenic mice. We found that repetitive intramuscular transplantation of hUCB-MSCs inhibited severe muscle atrophy (Figure 2.3.1 and 2.3.5). We also found that improvement in pathology is associated with regulation of ROS and

RNS. In addition, we showed that hUCB-MSCs increased protein synthesis and protein level expression of AMPK in C2C12 myotubes and skeletal muscle of SOD1 transgenic mice (Figure 2.3.3 and 2.3.6). As a result, the protective effect of hUCB-MSCs in skeletal muscle of transgenic mice might be related to AMPK and oxidative stress.

In previous studies, activation of AMPK in skeletal muscle led to different outcomes. Metformin, an activator of AMPK, reduced the rate of protein synthesis. However, the activators of AMPK, AICAR and A-769662, increased protein synthesis (Hall et al., 2018). These evidences suggested that activation of AMPK might restore or inhibit protein synthesis in skeletal muscle depend on inducer or activator. To confirm that the activation of AMPK induced by hUCB-MSCs is related to protein synthesis, we investigated the protein levels of S6K in C2C12 myotubes and skeletal muscle of SOD1 transgenic mice, and found that hUCB-MSCs increased S6K protein levels (Figure 2.3.3 and 2.3.6). These results suggest that the activation of AMPK induced by hUCB-MSCs has a positive effect on skeletal muscle such as AICAR or A-769662. In line with this, the activation of AMPK induced by hUCB-MSCs ameliorate skeletal muscle pathology through iNOS/NO and protein synthesis. It has also been shown that hUCB-mSCs decreased ROS as in previous studies (Powers, Ji, Kavazis, & Jackson, 2011; Schieber & Chandel, 2014).

In this report, we showed that hUCB-MSCs ameliorated muscle atrophy and restored NMJs through inhibition of ROS in C2C12 cells and skeletal muscle. Additionally, hUCB-MSCs increased protein synthesis and suppressed iNOS/NO levels in skeletal muscle. In conclusion, repeated transplantation of hUCB-MSCs into the skeletal muscle of hSOD1-G93A mice prolonged survival and increased motor activity in hSOD1-G93A mice, and these results suggest that hUCB-MSCs are a potential therapeutic strategy for ALS.

GENERAL CONCLUSION

ALS is a fatal neurodegenerative disease. During disease progression, motor neurons are selectively death and cause many pathological conditions including rigidity and muscle atrophy. Although many clinical trials have been tried and showed safety and beneficial effects, but there are no effective therapy for patients with ALS. Therefore, there are needs to find new therapeutic options and mechanism for effective therapy in the field of clinics.

In this study, I suggest two therapeutic options, CAM and hUCB-MSCs. Although two options are quite different, they showed similar therapeutic mechanism in the different cell types and provided significant therapeutic efficacy in SOD1 transgenic mice. Therefor this study suggest two beneficial and effective therapeutic options for patients with ALS.

In the first study, I revealed that the oral administration of KCHO-1 for one month showed beneficial effects in survival rate and motor function in SOD1 transgenic mice. Moreover, KCHO-1 reduced oxidative stress in BV2 activated microglial cells and inhibition of activated microglial cells was also showed in SOD1 transgenic mice model. KCHO-1 inhibit oxidative stress via reduction of NOX2 expression. Therefore, this study provide novel

therapeutic option and specific mechanism for clinical trials of ALS.

In the second study, I investigated the therapeutic potential of hUCB-MSCs against ALS. hUCB-MSCs have been used in many clinical trials and showed beneficial effect for several disease including ALS. However, there are no study for identify the specific mechanism by using hUCB-MSC with intramuscular route in ALS patients. Therefore, in this study we demonstrate that the repeated intramuscular transplantation of hUCB-MSCs exhibited significant beneficial effect on SOD1 transgenic mice. Particularly, hUCB-MSCs efficiently modulate protein synthesis and cell survival pathway by targeting AMPK signaling. Therefore, this study suggest the possibility of hCUB-MSCs as a cell therapy and provide a novel therapeutic route for ALS patients.

Consequently, I anticipate that these results could provide beneficial therapeutic options and bring new insights for the clinical trials and treatment of patients with ALS.

2.5 REFEFENCE

Abrigo, J., Rivera, J. C., Simon, F., Cabrera, D., & Cabello-Verrugio, C. (2016). Transforming growth factor type beta (TGF-beta) requires reactive oxygen species to induce skeletal muscle atrophy. *Cell Signal, 28*(5), 366-376. doi:10.1016/j.cellsig.2016.01.010

Abrigo, J., Simon, F., Cabrera, D., & Cabello-Verrugio, C. (2016). Angiotensin-(1-7) Prevents Skeletal Muscle Atrophy Induced by Transforming Growth Factor Type Beta (TGF-beta) via Mas Receptor Activation. *Cell Physiol Biochem, 40*(1-2), 27-38. doi:10.1159/000452522

Apolloni, S., Parisi, C., Pesaresi, M. G., Rossi, S., Carri, M. T., Cozzolino, M., . . . D'Ambrosi, N. (2013). The NADPH oxidase pathway is dysregulated by the P2X7 receptor in the SOD1-G93A microglia model of amyotrophic lateral sclerosis. *J Immunol, 190*(10), 5187-5195. doi:10.4049/jimmunol.1203262

Bak, D. H., Na, J., Im, S. I., Oh, C. T., Kim, J. Y., Park, S. K., . . . Kim, B. J. (2019). Antioxidant effect of human placenta hydrolysate against oxidative stress on muscle atrophy. *Journal of Cellular Physiology, 234*(2), 1643-1658. doi:10.1002/jcp.27034

Baloh, R. H., Glass, J. D., & Svendsen, C. N. (2018). Stem cell transplantation for amyotrophic lateral sclerosis. *Curr Opin Neurol, 31*(5), 655-661. doi:10.1097/WCO.0000000000000598

Barber, S. C., & Shaw, P. J. (2010). Oxidative stress in ALS: key role in motor neuron injury and therapeutic target. *Free Radic Biol Med, 48*(5), 629-641. doi:10.1016/j.freeradbiomed.2009.11.018

Ben Haim, L., Carrillo-de Sauvage, M. A., Ceyzeriat, K., & Escartin, C. (2015). Elusive roles for reactive astrocytes in neurodegenerative diseases. *Front Cell Neurosci, 9*, 278. doi:10.3389/fncel.2015.00278

Boillee, S., & Cleveland, D. W. (2008). Revisiting oxidative damage in ALS: microglia, Nox, and mutant SOD1. *J Clin Invest, 118*(2), 474-478. doi:10.1172/JCI34613

Bordt, E. A., & Polster, B. M. (2014). NADPH oxidase- and mitochondria-derived reactive oxygen species in proinflammatory microglial activation: a bipartisan affair? *Free Radic Biol Med, 76*, 34-46. doi:10.1016/j.freeradbiomed.2014.07.033

Bozzo, F., Mirra, A., & Carri, M. T. (2016). Oxidative stress and mitochondrial damage in the pathogenesis of ALS: New perspectives. *Neurosci Lett*. doi:10.1016/j.neulet.2016.04.065

Brown, G. C., & Neher, J. J. (2010). Inflammatory neurodegeneration and

mechanisms of microglial killing of neurons. *Mol Neurobiol, 41*(2-3), 242-247. doi:10.1007/s12035-010-8105-9

Bucchia, M., Ramirez, A., Parente, V., Simone, C., Nizzardo, M., Magri, F., . . . Corti, S. (2015). Therapeutic Development in Amyotrophic Lateral Sclerosis. *Clin Ther*. doi:10.1016/j.clinthera.2014.12.020

Cai, M., Lee, S. H., & Yang, E. J. (2019). Bojungikgi-tang Improves Muscle and Spinal Cord Function in an Amyotrophic Lateral Sclerosis Model. *Molecular Neurobiology, 56*(4), 2394-2407. doi:10.1007/s12035-018-1236-0

Cai, M., & Yang, E. J. (2019). Complementary and alternative medicine for treating amyotrophic lateral sclerosis: A narrative review. *Integr Med Res, 8*(4), 234-239. doi:10.1016/j.imr.2019.08.003

Casas, C., Manzano, R., Vaz, R., Osta, R., & Brites, D. (2016). Synaptic Failure: Focus in an Integrative View of ALS. *Brain Plast, 1*(2), 159-175. doi:10.3233/BPL-140001

Chen, H., Kankel, M. W., Su, S. C., Han, S. W. S., & Ofengeim, D. (2018). Exploring the genetics and non-cell autonomous mechanisms underlying ALS/FTLD. *Cell Death Differ, 25*(4), 648-662. doi:10.1038/s41418-018-0060-4

Chia, R., Chio, A., & Traynor, B. J. (2018). Novel genes associated with amyotrophic lateral sclerosis: diagnostic and clinical implications. *Lancet Neurol, 17*(1), 94-102. doi:10.1016/S1474-4422(17)30401-5

Ciervo, Y., Ning, K., Jun, X., Shaw, P. J., & Mead, R. J. (2017). Advances, challenges and future directions for stem cell therapy in amyotrophic lateral sclerosis. *Mol Neurodegener, 12*(1), 85. doi:10.1186/s13024-017-0227-3

Cifra, A., Mazzone, G. L., & Nistri, A. (2013). Riluzole: What It Does to Spinal and Brainstem Neurons and How It Does It. *Neuroscientist, 19*(2), 137-144. doi:10.1177/1073858412444932

Coughlan, K. S., Mitchem, M. R., Hogg, M. C., & Prehn, J. H. M. (2015). "Preconditioning" with latrepirdine, an adenosine 5 '-monophosphate-activated protein kinase activator, delays amyotrophic lateral sclerosis progression in SOD1(G93A) mice. *Neurobiology of Aging, 36*(2), 1140-1150. doi:10.1016/j.neurobiolaging.2014.09.022

Di Giorgio, F. P., Carrasco, M. A., Siao, M. C., Maniatis, T., & Eggan, K. (2007). Non-cell autonomous effect of glia on motor neurons in an embryonic stem cell-based ALS model. *Nat Neurosci, 10*(5), 608-614. doi:10.1038/nn1885

Di Pietro, L., Baranzini, M., Berardinelli, M. G., Lattanzi, W., Monforte, M., Tasca, G., . . . Bernardini, C. (2017). Potential therapeutic targets for ALS: MIR206, MIR208b and MIR499 are modulated during disease progression in the skeletal muscle of patients. *Sci Rep, 7*(1), 9538. doi:10.1038/s41598-017-10161-z

Dial, A. G., Ng, S. Y., Manta, A., & Ljubicic, V. (2018). The Role of AMPK in Neuromuscular Biology and Disease. *Trends Endocrinol Metab, 29*(5), 300-312. doi:10.1016/j.tem.2018.02.010

Du, H., Wu, J., Li, H., Zhong, P. X., Xu, Y. J., Li, C. H., . . . Wang, L. S. (2013). Polyphenols and triterpenes from Chaenomeles fruits: chemical analysis and antioxidant activities assessment. *Food Chem, 141*(4), 4260-4268. doi:10.1016/j.foodchem.2013.06.109

Dupuis, L., Gonzalez de Aguilar, J. L., Echaniz-Laguna, A., Eschbach, J., Rene, F., Oudart, H., . . . Loeffler, J. P. (2009). Muscle mitochondrial uncoupling dismantles neuromuscular junction and triggers distal degeneration of motor neurons. *PLoS One, 4*(4), e5390. doi:10.1371/journal.pone.0005390

Falci, L., Shi, Z. X., & Greenlee, H. (2016). Multiple Chronic Conditions and Use of Complementary and Alternative Medicine Among US Adults: Results From the 2012 National Health Interview Survey. *Preventing Chronic Disease, 13*. doi:ARTN E61
10.5888/pcd13.150501

Fischer, L. R., Culver, D. G., Tennant, P., Davis, A. A., Wang, M. S., Castellano-Sanchez, A., . . . Glass, J. D. (2004). Amyotrophic lateral sclerosis is a distal axonopathy: evidence in mice and man. *Experimental Neurology, 185*(2), 232-240. doi:10.1016/j.expneurol.2003.10.004

Forostyak, S., Homola, A., Turnovcova, K., Svitil, P., Jendelova, P., & Sykova, E. (2014). Intrathecal delivery of mesenchymal stromal cells protects the structure of altered perineuronal nets in SOD1 rats and amends the course of ALS. *Stem Cells, 32*(12), 3163-3172. doi:10.1002/stem.1812

Geloso, M. C., Corvino, V., Marchese, E., Serrano, A., Michetti, F., & D'Ambrosi, N. (2017). The Dual Role of Microglia in ALS: Mechanisms and Therapeutic Approaches. *Front Aging Neurosci, 9*, 242. doi:10.3389/fnagi.2017.00242

Gugliandolo, A., Bramanti, P., & Mazzon, E. (2019). Mesenchymal Stem Cells: A Potential Therapeutic Approach for Amyotrophic Lateral Sclerosis? *Stem Cells Int, 2019*, 3675627. doi:10.1155/2019/3675627

Hall, D. T., Griss, T., Ma, J. F., Sanchez, B. J., Sadek, J., Tremblay, A. M. K., . . . Gallouzi, I. E. (2018). The AMPK agonist 5-aminoimidazole-4-carboxamide ribonucleotide (AICAR), but not metformin, prevents inflammation-associated cachectic muscle wasting. *Embo Molecular Medicine, 10*(7). doi:UNSP e8307
10.15252/emmm.201708307

Hardiman, O., Al-Chalabi, A., Chio, A., Corr, E. M., Logroscino, G., Robberecht, W., . . . van den Berg, L. H. (2017). Amyotrophic lateral sclerosis. *Nat Rev Dis Primers, 3*, 17085. doi:10.1038/nrdp.2017.85

Ho, M. S. (2019). Microglia in Parkinson's Disease. *Adv Exp Med Biol, 1175*, 335-353. doi:10.1007/978-981-13-9913-8_13

Hong, J. A., Chung, S. H., Lee, J. S., Kim, S. S., Shin, H. D., Kim, H., . . . Kim, C. J. (2003). Effects of Paeonia radix on 5-hydroxytryptamine synthesis and tryptophan hydroxylase expression in the dorsal raphe of exercised rats. *Biol Pharm Bull, 26*(2), 166-169.

Hong, M. H., Kim, J. H., Bae, H., Lee, N. Y., Shin, Y. C., Kim, S. H., & Ko, S. G. (2010). Atractylodes japonica Koidzumi inhibits the production of proinflammatory cytokines through inhibition of the NF-kappaB/IkappaB signal pathway in HMC-1 human mast cells. *Arch Pharm Res, 33*(6), 843-851. doi:10.1007/s12272-010-0606-6

Hooten, K. G., Beers, D. R., Zhao, W., & Appel, S. H. (2015). Protective and Toxic Neuroinflammation in Amyotrophic Lateral Sclerosis. *Neurotherapeutics*. doi:10.1007/s13311-014-0329-3

Huai, J., & Zhang, Z. (2019). Structural Properties and Interaction Partners of Familial ALS-Associated SOD1 Mutants. *Front Neurol, 10*, 527. doi:10.3389/fneur.2019.00527

Ichim, T. E., Alexandrescu, D. T., Solano, F., Lara, F., Campion Rde, N., Paris, E., . . . Riordan, N. H. (2010). Mesenchymal stem cells as anti-inflammatories: implications for treatment of Duchenne muscular dystrophy. *Cell Immunol, 260*(2), 75-82. doi:10.1016/j.cellimm.2009.10.006

Islam, M. T. (2017). Oxidative stress and mitochondrial dysfunction-linked neurodegenerative disorders. *Neurol Res, 39*(1), 73-82. doi:10.1080/01616412.2016.1251711

Jaiswal, M. K. (2019). Riluzole and edaravone: A tale of two amyotrophic lateral sclerosis drugs. *Med Res Rev, 39*(2), 733-748. doi:10.1002/med.21528

Jeong, H., Lee, J., Cha, E., Park, M., Son, I., Song, B., & Kim, S. (2014). A study on the oral toxicity of mecasin in rats. *J Pharmacopuncture, 17*(4), 61-65. doi:10.3831/KPI.2014.17.038

Jiang, J., & Ravits, J. (2019). Pathogenic Mechanisms and Therapy Development for C9orf72 Amyotrophic Lateral Sclerosis/Frontotemporal Dementia. *Neurotherapeutics, 16*(4), 1115-1132. doi:10.1007/s13311-019-00797-2

Jiang, W. Y., Jeon, B. H., Kim, Y. C., Lee, S. H., Sohn, D. H., & Seo, G. S. (2013). PF2401-SF, standardized fraction of Salvia miltiorrhiza shows anti-inflammatory activity in macrophages and acute arthritis in vivo. *Int Immunopharmacol, 16*(2), 160-164. doi:10.1016/j.intimp.2013.03.028

Kaneb, H. M., Sharp, P. S., Rahmani-Kondori, N., & Wells, D. J. (2011). Metformin Treatment Has No Beneficial Effect in a Dose-Response Survival Study in the SOD1(G93A) Mouse Model of ALS and Is Harmful in Female Mice. *PLoS One, 6*(9). doi:ARTN e24189

10.1371/journal.pone.0024189
Kim, B. W., Koppula, S., Kim, J. W., Lim, H. W., Hwang, J. W., Kim, I. S., . . . Choi, D. K. (2012). Modulation of LPS-stimulated neuroinflammation in BV-2 microglia by Gastrodia elata: 4-hydroxybenzyl alcohol is the bioactive candidate. *J Ethnopharmacol, 139*(2), 549-557. doi:10.1016/j.jep.2011.11.048
Kim, E. K., & Choi, E. J. (2010). Pathological roles of MAPK signaling pathways in human diseases. *Biochim Biophys Acta, 1802*(4), 396-405. doi:10.1016/j.bbadis.2009.12.009
Kim, G., Gautier, O., Tassoni-Tsuchida, E., Ma, X. R., & Gitler, A. D. (2020). ALS Genetics: Gains, Losses, and Implications for Future Therapies. *Neuron*. doi:10.1016/j.neuron.2020.08.022
Kim, K. S., Lee, D. S., Bae, G. S., Park, S. J., Kang, D. G., Lee, H. S., . . . Kim, Y. C. (2013). The inhibition of JNK MAPK and NF-kappaB signaling by tenuifoliside A isolated from Polygala tenuifolia in lipopolysaccharide-induced macrophages is associated with its anti-inflammatory effect. *Eur J Pharmacol, 721*(1-3), 267-276. doi:10.1016/j.ejphar.2013.09.026
Kim, Y., You, Y., Yoon, H. G., Lee, Y. H., Kim, K., Lee, J., . . . Jun, W. (2014). Hepatoprotective effects of fermented Curcuma longa L. on carbon tetrachloride-induced oxidative stress in rats. *Food Chem, 151*, 148-153. doi:10.1016/j.foodchem.2013.11.058
Kjaeldgaard, A. L., Pilely, K., Olsen, K. S., Pedersen, S. W., Lauritsen, A. O., Moller, K., & Garred, P. (2018). Amyotrophic lateral sclerosis: The complement and inflammatory hypothesis. *Mol Immunol, 102*, 14-25. doi:10.1016/j.molimm.2018.06.007
Kobayashi, K., Imagama, S., Ohgomori, T., Hirano, K., Uchimura, K., Sakamoto, K., . . . Kadomatsu, K. (2013). Minocycline selectively inhibits M1 polarization of microglia. *Cell Death Dis, 4*, e525. doi:10.1038/cddis.2013.54
Kumar, A., Barrett, J. P., Alvarez-Croda, D. M., Stoica, B. A., Faden, A. I., & Loane, D. J. (2016). NOX2 drives M1-like microglial/macrophage activation and neurodegeneration following experimental traumatic brain injury. *Brain Behav Immun, 58*, 291-309. doi:10.1016/j.bbi.2016.07.158
Lee, D. S., Ko, W., Song, B. K., Son, I., Kim, D. W., Kang, D. G., . . . Kim, S. (2016). The herbal extract KCHO-1 exerts a neuroprotective effect by ameliorating oxidative stress via heme oxygenase-1 upregulation. *Mol Med Rep, 13*(6), 4911-4919. doi:10.3892/mmr.2016.5129
Lee, D. S., Ko, W., Yoon, C. S., Kim, D. C., Yun, J., Lee, J. K., . . . Kim, Y. C. (2014). KCHO-1, a Novel Antineuroinflammatory Agent, Inhibits Lipopolysaccharide-Induced Neuroinflammatory Responses through Nrf2-Mediated Heme Oxygenase-1 Expression in Mouse BV2 Microglia Cells. *Evid Based Complement Alternat Med, 2014*, 357154.

doi:10.1155/2014/357154
Lee, S. H., & Yang, E. J. (2019). Anti-Neuroinflammatory Effect of Jaeumganghwa-Tang in an Animal Model of Amyotrophic Lateral Sclerosis. *Evidence-Based Complementary and Alternative Medicine*. doi:Artn 1893526
10.1155/2019/1893526
Lepore, E., Casola, I., Dobrowolny, G., & Musaro, A. (2019). Neuromuscular Junction as an Entity of Nerve-Muscle Communication. *Cells, 8*(8). doi:ARTN 906
10.3390/cells8080906
Liao, B., Zhao, W., Beers, D. R., Henkel, J. S., & Appel, S. H. (2012). Transformation from a neuroprotective to a neurotoxic microglial phenotype in a mouse model of ALS. *Exp Neurol, 237*(1), 147-152. doi:10.1016/j.expneurol.2012.06.011
Lim, M. A., Selak, M. A., Xiang, Z., Krainc, D., Neve, R. L., Kraemer, B. C., . . . Kalb, R. G. (2012). Reduced activity of AMP-activated protein kinase protects against genetic models of motor neuron disease. *J Neurosci, 32*(3), 1123-1141. doi:10.1523/JNEUROSCI.6554-10.2012
Liu, Y. J., Ju, T. C., Chen, H. M., Jang, Y. S., Lee, L. M., Lai, H. L., . . . Chern, Y. (2015). Activation of AMP-activated protein kinase alpha1 mediates mislocalization of TDP-43 in amyotrophic lateral sclerosis. *Hum Mol Genet, 24*(3), 787-801. doi:10.1093/hmg/ddu497
Liu, Y. J., Lee, L. M., Lai, H. L., & Chern, Y. (2015). Aberrant activation of AMP-activated protein kinase contributes to the abnormal distribution of HuR in amyotrophic lateral sclerosis. *FEBS Lett, 589*(4), 432-439. doi:10.1016/j.febslet.2014.12.029
Loeffler, J. P., Picchiarelli, G., Dupuis, L., & Gonzalez De Aguilar, J. L. (2016). The Role of Skeletal Muscle in Amyotrophic Lateral Sclerosis. *Brain Pathol, 26*(2), 227-236. doi:10.1111/bpa.12350
Lunn, J. S., Sakowski, S. A., & Feldman, E. L. (2014). Concise review: Stem cell therapies for amyotrophic lateral sclerosis: recent advances and prospects for the future. *Stem Cells, 32*(5), 1099-1109. doi:10.1002/stem.1628
Manavalan, A., Ramachandran, U., Sundaramurthi, H., Mishra, M., Sze, S. K., Hu, J. M., . . . Heese, K. (2012). Gastrodia elata Blume (tianma) mobilizes neuro-protective capacities. *Int J Biochem Mol Biol, 3*(2), 219-241.
Mancuso, R., del Valle, J., Modol, L., Martinez, A., Granado-Serrano, A. B., Ramirez-Nunez, O., . . . Navarro, X. (2014). Resveratrol improves motoneuron function and extends survival in SOD1(G93A) ALS mice. *Neurotherapeutics, 11*(2), 419-432. doi:10.1007/s13311-013-0253-y
Marden, J. J., Harraz, M. M., Williams, A. J., Nelson, K., Luo, M., Paulson, H.,

& Engelhardt, J. F. (2007). Redox modifier genes in amyotrophic lateral sclerosis in mice. *J Clin Invest, 117*(10), 2913-2919. doi:10.1172/JCI31265

Mazzini, L., Fagioli, F., Boccaletti, R., Mareschi, K., Oliveri, G., Olivieri, C., . . . Madon, E. (2003). Stem cell therapy in amyotrophic lateral sclerosis: a methodological approach in humans. *Amyotroph Lateral Scler Other Motor Neuron Disord, 4*(3), 158-161. doi:10.1080/14660820310014653

Mejzini, R., Flynn, L. L., Pitout, I. L., Fletcher, S., Wilton, S. D., & Akkari, P. A. (2019). ALS Genetics, Mechanisms, and Therapeutics: Where Are We Now? *Front Neurosci, 13*, 1310. doi:10.3389/fnins.2019.01310

Miller, R. G., Mitchell, J. D., & Moore, D. H. (2012). Riluzole for amyotrophic lateral sclerosis (ALS)/motor neuron disease (MND). *Cochrane Database Syst Rev*(3), CD001447. doi:10.1002/14651858.CD001447.pub3

Mungrue, I. N., Husain, M., & Stewart, D. J. (2002). The role of NOS in heart failure: lessons from murine genetic models. *Heart Fail Rev, 7*(4), 407-422.

Oh, K. W., Noh, M. Y., Kwon, M. S., Kim, H. Y., Oh, S. I., Park, J., . . . Kim, S. H. (2018). Repeated Intrathecal Mesenchymal Stem Cells for Amyotrophic Lateral Sclerosis. *Ann Neurol, 84*(3), 361-373. doi:10.1002/ana.25302

Palomo, G. M., & Manfredi, G. (2015). Exploring new pathways of neurodegeneration in ALS: The role of mitochondria quality control. *Brain Res, 1607*, 36-46. doi:10.1016/j.brainres.2014.09.065

Park, C. M., Kim, M. J., Kim, S. M., Park, J. H., Kim, Z. H., & Choi, Y. S. (2016). Umbilical cord mesenchymal stem cell-conditioned media prevent muscle atrophy by suppressing muscle atrophy-related proteins and ROS generation. *In Vitro Cell Dev Biol Anim, 52*(1), 68-76. doi:10.1007/s11626-015-9948-1

Park, S., & Yang, E. J. (2018). Anti-Inflammatory Effect of Gamisoyo-San in an Animal Model of Amyotrophic Lateral Sclerosis. *Evidence-Based Complementary and Alternative Medicine*. doi:Artn 8580152
10.1155/2018/8580152

Perera, N. D., Sheean, R. K., Scott, J. W., Kemp, B. E., Horne, M. K., & Turner, B. J. (2014). Mutant TDP-43 Deregulates AMPK Activation by PP2A in ALS Models. *PLoS One, 9*(3). doi:ARTN e90449
10.1371/journal.pone.0090449

Perera, N. D., & Turner, B. J. (2016). AMPK Signalling and Defective Energy Metabolism in Amyotrophic Lateral Sclerosis. *Neurochem Res, 41*(3), 544-553. doi:10.1007/s11064-015-1665-3

Petrou, P., Gothelf, Y., Argov, Z., Gotkine, M., Levy, Y. S., Kassis, I., . . . Karussis, D. (2016). Safety and Clinical Effects of Mesenchymal Stem Cells Secreting Neurotrophic Factor Transplantation in

Patients With Amyotrophic Lateral Sclerosis: Results of Phase 1/2 and 2a Clinical Trials. *JAMA Neurol, 73*(3), 337-344. doi:10.1001/jamaneurol.2015.4321

Pollari, E., Goldsteins, G., Bart, G., Koistinaho, J., & Giniatullin, R. (2014). The role of oxidative stress in degeneration of the neuromuscular junction in amyotrophic lateral sclerosis. *Front Cell Neurosci, 8*, 131. doi:10.3389/fncel.2014.00131

Powers, S. K., Ji, L. L., Kavazis, A. N., & Jackson, M. J. (2011). Reactive oxygen species: impact on skeletal muscle. *Compr Physiol, 1*(2), 941-969. doi:10.1002/cphy.c100054

Rehorova, M., Vargova, I., Forostyak, S., Vackova, I., Turnovcova, K., Kupcova Skalnikova, H., . . . Jendelova, P. (2019). A Combination of Intrathecal and Intramuscular Application of Human Mesenchymal Stem Cells Partly Reduces the Activation of Necroptosis in the Spinal Cord of SOD1(G93A) Rats. *Stem Cells Transl Med*. doi:10.1002/sctm.18-0223

Sahni, V., & Kessler, J. A. (2010). Stem cell therapies for spinal cord injury. *Nat Rev Neurol, 6*(7), 363-372. doi:10.1038/nrneurol.2010.73

Samuel, M. A., Voinescu, P. E., Lilley, B. N., de Cabo, R., Foretz, M., Viollet, B., . . . Sanes, J. R. (2014). LKB1 and AMPK regulate synaptic remodeling in old age. *Nat Neurosci, 17*(9), 1190-1197. doi:10.1038/nn.3772

Sancheti, S., Sancheti, S., & Seo, S. Y. (2013). Antidiabetic and antiacetylcholinesterase effects of ethyl acetate fraction of Chaenomeles sinensis (Thouin) Koehne fruits in streptozotocin-induced diabetic rats. *Exp Toxicol Pathol, 65*(1-2), 55-60. doi:10.1016/j.etp.2011.05.010

Schieber, M., & Chandel, N. S. (2014). ROS function in redox signaling and oxidative stress. *Curr Biol, 24*(10), R453-462. doi:10.1016/j.cub.2014.03.034

Shin, S. J., Kim, D., Kim, J. S., Kim, I., Lee, J. R., Kim, S. C., & Kim, B. J. (2018). Effects of Gamisoyo-San Decoction, a Traditional Chinese Medicine, on Gastrointestinal Motility. *Digestion, 98*(4), 231-237. doi:10.1159/000489455

Singh, A., Kukreti, R., Saso, L., & Kukreti, S. (2019). Oxidative Stress: A Key Modulator in Neurodegenerative Diseases. *Molecules, 24*(8). doi:10.3390/molecules24081583

Smith, E. F., Shaw, P. J., & De Vos, K. J. (2019). The role of mitochondria in amyotrophic lateral sclerosis. *Neurosci Lett, 710*, 132933. doi:10.1016/j.neulet.2017.06.052

Suzuki, M., McHugh, J., Tork, C., Shelley, B., Hayes, A., Bellantuono, I., . . . Svendsen, C. N. (2008). Direct muscle delivery of GDNF with human mesenchymal stem cells improves motor neuron survival and function in a rat model of familial ALS. *Mol Ther, 16*(12), 2002-2010.

doi:10.1038/mt.2008.197
Sykova, E., Rychmach, P., Drahoradova, I., Konradova, S., Ruzickova, K., Vorisek, I., . . . Bojar, M. (2017). Transplantation of Mesenchymal Stromal Cells in Patients With Amyotrophic Lateral Sclerosis: Results of Phase I/IIa Clinical Trial. *Cell Transplant, 26*(4), 647-658. doi:10.3727/096368916X693716
Takeuchi, A., Isobe, K. I., Miyaishi, O., Sawada, M., Fan, Z. H., Nakashima, I., & Kiuchi, K. (1998). Microglial NO induces delayed neuronal death following acute injury in the striatum. *Eur J Neurosci, 10*(5), 1613-1620.
Tang, Y., & Le, W. (2016). Differential Roles of M1 and M2 Microglia in Neurodegenerative Diseases. *Molecular Neurobiology, 53*(2), 1181-1194. doi:10.1007/s12035-014-9070-5
Tarafdar, A., & Pula, G. (2018). The Role of NADPH Oxidases and Oxidative Stress in Neurodegenerative Disorders. *Int J Mol Sci, 19*(12). doi:10.3390/ijms19123824
Tsitkanou, S., Della Gatta, P. A., & Russell, A. P. (2016). Skeletal Muscle Satellite Cells, Mitochondria, and MicroRNAs: Their Involvement in the Pathogenesis of ALS. *Front Physiol, 7*, 403. doi:10.3389/fphys.2016.00403
Van Damme, P., Robberecht, W., & Van Den Bosch, L. (2017). Modelling amyotrophic lateral sclerosis: progress and possibilities. *Dis Model Mech, 10*(5), 537-549. doi:10.1242/dmm.029058
Villinski, J. R., Bergeron, C., Cannistra, J. C., Gloer, J. B., Coleman, C. M., Ferreira, D., . . . Gafner, S. (2014). Pyrano-isoflavans from Glycyrrhiza uralensis with antibacterial activity against Streptococcus mutans and Porphyromonas gingivalis. *J Nat Prod, 77*(3), 521-526. doi:10.1021/np400788r
Wang, G. Y., Rayner, S. L., Chung, R., Shi, B. Y., & Liang, X. J. (2020). Advances in nanotechnology-based strategies for the treatments of amyotrophic lateral sclerosis. *Mater Today Bio, 6*, 100055. doi:10.1016/j.mtbio.2020.100055
Wasner, M., Klier, H., & Borasio, G. D. (2001). The use of alternative medicine by patients with amyotrophic lateral sclerosis. *Journal of the Neurological Sciences, 191*(1-2), 151-154. doi:Doi 10.1016/S0022-510x(01)00615-3
Weishaupt, J. H., Hyman, T., & Dikic, I. (2016). Common Molecular Pathways in Amyotrophic Lateral Sclerosis and Frontotemporal Dementia. *Trends Mol Med, 22*(9), 769-783. doi:10.1016/j.molmed.2016.07.005
Wu, D. C., Re, D. B., Nagai, M., Ischiropoulos, H., & Przedborski, S. (2006). The inflammatory NADPH oxidase enzyme modulates motor neuron degeneration in amyotrophic lateral sclerosis mice. *Proc Natl Acad Sci U S A, 103*(32), 12132-12137. doi:10.1073/pnas.0603670103

Xiao, Y., Karam, C., Yi, J., Zhang, L., Li, X., Yoon, D., . . . Zhou, J. (2018). ROS-related mitochondrial dysfunction in skeletal muscle of an ALS mouse model during the disease progression. *Pharmacol Res, 138*, 25-36. doi:10.1016/j.phrs.2018.09.008

Xu, H., Arita, H., Hayashida, M., Zhang, L., Sekiyama, H., & Hanaoka, K. (2006). Pain-relieving effects of processed Aconiti tuber in CCI-neuropathic rats. *J Ethnopharmacol, 103*(3), 392-397. doi:10.1016/j.jep.2005.08.050

Yang, E. J., Jiang, J. H., Lee, S. M., Yang, S. C., Hwang, H. S., Lee, M. S., & Choi, S. M. (2010). Bee venom attenuates neuroinflammatory events and extends survival in amyotrophic lateral sclerosis models. *J Neuroinflammation, 7*, 69. doi:10.1186/1742-2094-7-69

Zhang, F., & Jiang, L. (2015). Neuroinflammation in Alzheimer's disease. *Neuropsychiatr Dis Treat, 11*, 243-256. doi:10.2147/NDT.S75546

Zhao, W., Beers, D. R., & Appel, S. H. (2013). Immune-mediated mechanisms in the pathoprogression of amyotrophic lateral sclerosis. *J Neuroimmune Pharmacol, 8*(4), 888-899. doi:10.1007/s11481-013-9489-x

Zhou, Q. M., Wang, Y. J., Zhang, J. J., Shao, Y. P., Li, S., Wang, Y., . . . Le, W. D. (2018). Fingerprint analysis of Huolingshengji Formula and its neuroprotective effects in SOD1(G93A) mouse model of amyotrophic lateral sclerosis. *Scientific Reports, 8*. doi:ARTN 1668
10.1038/s41598-018-19923-9

Zou, Z. Y., Zhou, Z. R., Che, C. H., Liu, C. Y., He, R. L., & Huang, H. P. (2017). Genetic epidemiology of amyotrophic lateral sclerosis: a systematic review and meta-analysis. *J Neurol Neurosurg Psychiatry, 88*(7), 540-549. doi:10.1136/jnnp-2016-315018

국문 초록

근위축성측삭경화증 동물모델에서 제대혈 유래 중간엽줄기세포와 허브 화합물의 신경보호효과에 관한 연구

서울대학교 대학원
수의학과
수의병인생물학 및 예방수의학 전공

국 명 근

(지도 교수: 강경선)

루게릭 질환이라고 알려진 측삭 경화증 (ALS) 은 상위 및 하위 운동성 신경세포가 선택적으로 사멸되는 신경퇴행성 질환으로서 이로 인하여

골격근내의 신경근 접합부가 소실 및 골격근퇴행 등 여러 장기에서 근위축이 발생하는 질환이다. 대부분의 루게릭 환자의 경우 산발성질환의 특성을 갖고 있으며, 대략 10%의 경우만이 가족성 루게릭 형태를 갖고 있다. 현재까지 루게릭 질환의 주요원인은 밝혀지지 않았지만, 이를 밝히기 위해 다양한 연구들이 진행되고 있으며, 특히 후생유전학 연구를 통하여 루게릭 질환과 연관이 있는 돌연변이 유전자들을 밝혀내고 있다. 그 중 가족성 루게릭 질환과 관련이 있는 활성산소 소거효소인 SOD1 유전자의 돌연변이 루게릭 질환 마우스 모델을 이용한 활발한 연구가 진행되고 있으며 이 외에도 FUS, TARDBP 및 C9orf72 등 루게릭의 원인을 밝히기 위한 다양한 연구가 지속되고 있다.

현재까지 환자 치료를 위해서 Riluzole 과 Edaravone 이 두 개의 약물만이 FDA로부터 승인을 받아 치료용으로 사용되고 있다. Riluzole의 경우 신경세포 내에서 과도한 글루탄산염의 분비를 억제함으로써 치료효과를 보여주고 있으며, Edaravone의 경우 과도한 활성산소를 억제함으로써 치료효과를 보여주고 있다. 하지만 임상결과 이 두 개의 약물을 사용했음에도 불구하고 평균적으로 3개월의 수명연장 효과만을 보여주고 있으며 아직 까지는 극적인 효과를 보이는 치료방법은 밝혀내지 못하고 있다. 이러한 문제를 극복하기 위해서 많은 연구들이 효과적인 치료제를 개발하기 위해 유전자치료, 화학적 치료 및 세포치료 등 다양한 시도가 진행되고 있다. 본 연구에서는 KCHO-1이라는 대체의학 약물과 제대혈 유래 중간엽 줄기세포를 이용하여 치료효과 및 이러한 치료제가 갖는 새로운 메커니즘을 검증하였다.

KCHO-1은 전통적으로 사용해온 여러 가지 약초들의 추출물을 혼합한 약초혼합물이다. KCHO-1의 효과를 검증하기 위해 돌연변이 SOD1

유전자를 보유하고 있는 쥐 모델을 이용하였고, 약 한 달간의 구강투여 결과 운동능력 및 생존기간에서 효과를 볼 수 있었다. 이러한 효과의 메커니즘을 확인하기 위해 루게릭 질환의 대표적인 질환 특성 중 하나인 활성산소의 농도를 확인하였고, 결과적으로 KCHO-1이 NOX2와 MAPK의 발현을 억제함으로써, 소교 세포 및 쥐 모델의 신경계 내에서 활성산소 농도를 줄여준다는 것을 확인할 수 있었다.

현재까지 신경퇴행성 질환을 치료하기 위해 다양한 세포치료가 시도되었다. 그 중에서 줄기세포를 이용한 치료는 가장 선호되는 방법 중 하나이며 기존의 임상실험 결과에서도 루게릭 질환에 신경보호효과가 있는 것이 알려진바 있다. 본 연구에서는 제대혈 유래 중간엽 줄기세포를 이용하여 돌연변이 SOD1 쥐 모델에서 효과를 확인하고자 했다. 이를 위해 우리는 제대혈 유래 중간엽 줄기세포를 쥐 모델의 골격근에 일주일에 한번씩 주기적으로 이식했다. 결과적으로 이식된 줄기세포는 쥐 모델의 운동능력 및 생존기간을 증가시켰을 뿐만 아니라, 골격근내의 활성산소의 축적을 줄여 줌으로써 골격근 및 신경근 접합부의 소실을 억제 했다. 특히, 이식된 제대혈 유래 중간엽 줄기세포는 골격근내의 AMPK 신호를 활성화 시키고, iNOS 신호를 억제했는데 이는 골격근내의 단백질 합성 신호를 촉진시키는 결과를 보여줬다.

이 연구 결과들은 (1) KCHO-1이라는 새로운 대체의학약물이 루게릭 질환 쥐 모델에서 신경계 내의 활성산소의 농도를 억제함으로써 효과가 있음을 확인했고, 이러한 효과가 소교 세포의 활성으로 인해 증가된 NOX2 신호를 억제함으로써 나타난다는 사실을 검증 했다. (2) 또한 제대혈 유래 중간엽 줄기세포를 기존의 신경계 경로가 아닌 골격근을 통한 경로를 통해 이식했을 때, 제대혈 유래 중간엽 줄기세포가 쥐 모델의 골

격근내의 AMPK 활성화 시키고 활성산소의 축적을 억제함으로써, 단백질 생성 촉진 및 iNOS 신호를 억제하여 쥐 모델의 골격근 및 신경근 접합부를 보호한다는 사실을 검증하였다. 결과적으로, 본 연구는 루게릭 질환에 대한 전도유망한 치료전략으로서 대체의학 약물인 KCHO-1 과 골격근 경로를 통한 제대혈 유래 중간엽 줄기세포의 적용 가능성에 대한 근거를 제시한다.

주요어: 신경퇴행성질환, 루게릭, 중간엽줄기세포, 대체의학, AMPK
학번: 2013-21544